MIXING AND BLENDING

1. Introduction

Fluid mixing is a unit operation carried out to reduce inhomogeneity of fluids in terms of concentration of components, physical properties, and temperature; and create dispersions of mutually insoluble phases. It is frequently encountered in the process industry where valuable products are manufactured through physical operations, mass-transfer, and reactions (Table 1). These industries include petroleum (qv), chemical, food, pharmaceutical, paints, waste water, cosmetic, paper (qv), and mineral processing. Improved mixing can translate to savings of several billions of dollars in these industries resulting from higher yield and selectivity, better product quality, reduced cost of separating impurities and faster product delivery to market. In some cases, mixing is critical to the success of key manufacturing steps thereby making processes competitive. The fundamental mechanism of mixing involves physical movement of material between various parts of the whole mass and creating shear. This is achieved by transmitting mechanical energy to force the fluid motion.

Mixing systems are broadly divided into single-phase systems involving miscible liquids, and multiphase systems such as solid–liquid, mutually insoluble liquids, and gas–liquid and gas–liquid–solid. Viscous liquids, solid–solid, pastes and heat-transfer systems are treated differently because of the need for unique equipment designs. This article discusses fundamental mixing concepts followed by four classes of mixing systems and different types of mixing equipment (Fig. 1). For each mixing system, information is provided on suitable mixer types along with design and scale-up issues.

These mixing systems offer high flexibility because they can be operated in batch, semibatch, or continuous modes. Adequate mixing is a prerequisite for the success of chemical processes in terms of minimizing investment and operating costs. In addition, chemical reactions with mass-transfer limitation can be enhanced to provide high yields. Good mixing, therefore, plays a significant role in the profitability of the process industry.

The desired mixing in a commercial process is achieved with different types of equipment, eg, agitators, jets, static mixers, air lifts. The design approach requires defining process mixing requirements; specifying mixer type and size, and other internals such as baffles; and designing mechanical components such as impeller blades, shaft, drive assembly, bearings, and supports.

2. Fundamental Concepts

2.1. Stirred Tank Geometries. A conventional mechanically agitated tank consists of a vertical vessel equipped with a top-entering rotating mixer. While the vessel cross-section can be square or rectangle, cylindrical configuration is most commonly used. The mixer package includes one or more impellers attached to a shaft that is connected to a gear box and a motor drive through a shaft seal, as shown in Figure 2. In cylindrical tanks, wall baffles must be used to prevent swirling of a low viscosity fluid that can result in surface vortexing,

Table 1. **Classes Mixing Applications**

Mixing Class	*Processes*
miscible liquids	Blending of lube oils, gasoline additives, dilution, chemical products, slow batch chemical reactions, fast reactions in in-line mixers, paint blending, cornstarch and syrup conversion and storage, pharmaceutical formulations.
liquid–solid	Preparing homogeneous slurries of light and heavy solids such as polymers, catalyst manufacture, dissolving solids, crystallization, solvent extraction, liquid–solid reactions, clay mixing and storage used in coatings and ceramics, mineral ore leaching, lime slaking and storage
immiscible liquids	Washing liquids with immiscible solvents, cosmetics, food products, alkylation, caustic treat of hydrocarbons, crude oil desalting, hydrolysis reactions, neutralization, extraction, suspension and emulsion polymerization, emulsions for personal care and pharmaceutical creams on ointments
gas–liquid	Absorption, stripping, oxidation, hydrogenation, oxonation of olefins, chlorination, gas scrubbing, steam heating of liquids, fermentation, aerobic waste water treatment
viscous liquids (Newtonian/non–Newtonian)	Blending polymer solutions, paints and pigments, Food products, solution and bulk polymerization deashing of catalyst from polymers
heat transfer	Heating and cooling through jackets and internal coils, temperature control for initiating and stopping chemical reactions

vapor entrainment, vibrations, and poor mixing. Baffles may not be needed in square and rectangular tanks because the corners can provide similar disruption of tangential flow. Baffles are also not used in blending of high viscosity liquids.

When using tall vessels, eg, flash drums and strippers, the mixer may be installed from the bottom to minimize the shaft length and provide higher

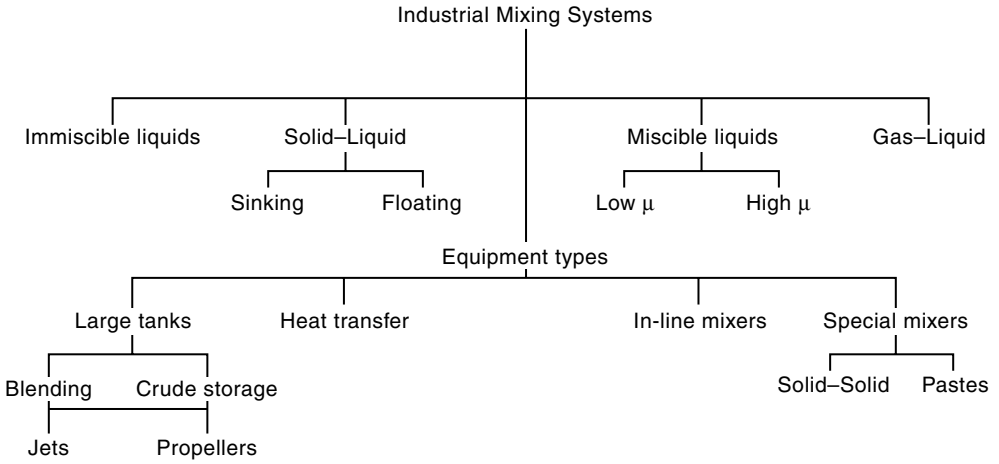

Fig. 1. Chart of industrial mixing systems.

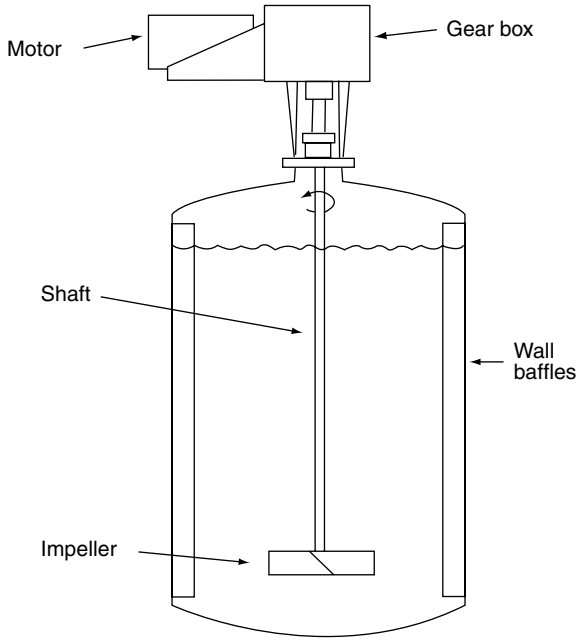

Fig. 2. Conventional stirred tank with top entering mixer.

mechanical stability (Fig. 3**a**). This design, however, is more prone to fluid leaks at the shaft seal and accumulation of solids if present in the process fluid. Mixers for very large product storage tanks are installed from the side near bottom (Fig. 3**b**). In horizontal cylindrical tanks, the mixer can be installed on the side or from top as shown in (Fig. 3**c** and **d**), respectively. The flow generated in these vessels (Fig. 3**b**–**d**) are asymmetric, and therefore wall baffles are not needed. However, off-center or angle mounting agitators are often used in small tanks to improve mixing.

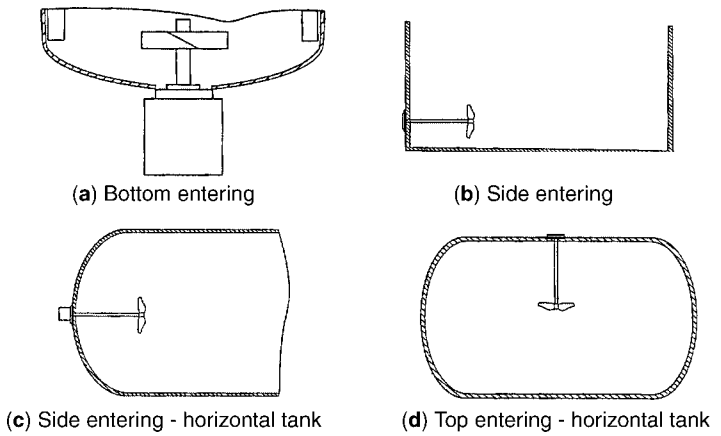

Fig. 3. Stirred tank geometries.

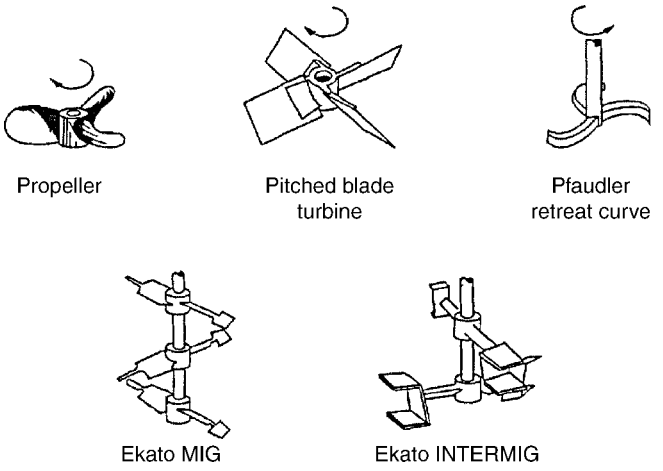

Fig. 4. Axial flow impellers.

2.2. Impeller Types. There are hundreds of impeller types marketed by vendors for a wide variety of commercial uses. Only the most common and general types will be discussed here. Selection of the most effective impeller should be based on understanding of process requirements, knowledge of fluid physical properties, and impeller characteristics. Impellers can be grouped as *turbines* suitable for low to medium viscosity fluids, and *close-clearance impellers* for high viscosity and complex fluids. Turbines are further characterized based on primary flow directions, eg, axial and radial. Within the axial flow family, hydrofoil impellers have been recently developed to increase flow at a cost of lower shear. There are also other specialty impeller designs developed for specific process needs such as very high shear.

Axial Flow Impellers (Fig. 4). Axial flow impellers pump fluid in the general direction parallel to the shaft, upward or downward. The downflow direction is effective for causing blending of miscible liquids and suspension of solids in liquids. The oldest axial flow impeller design is a marine propeller, which is often used as a side-entering mixer in large tanks and a top-entering mixer in small tanks. Because of its manufacture by casting, a propeller becomes very heavy when large and therefore is not commonly used as a top-entering mixer for tank sizes >5ft.

A pitched blade turbine (PBT) is fabricated by bolting on blades on a hub, and therefore is lighter than a propeller of same size. The blades can be at any angle, but the vast majority of PBTs have blades mounted at 45° angle with the horizontal. Angles <30° and >60° are extremely rare.

A retreat curve impeller was developed by the Pfaudler Company for glass lined reactors used for corrosive fluids. The new enamel coating technology permits the use of any impeller type for corrosive fluids. Glass-lined reactors can be easily cleaned, and therefore are most often used to avoid product contamination especially in pharmaceutical applications.

Two-bladed impellers, MIG and INTERMIG, were developed by the Ekato Company mainly for highly viscous fluids. These impellers are designed at high

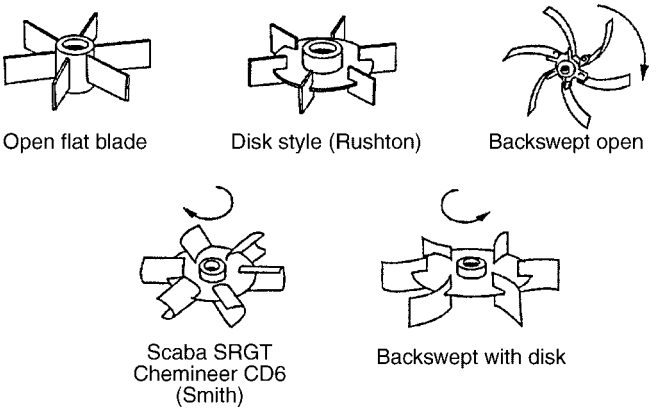

Fig. 5. Radial flow impellers.

impeller to tank diameter ratio ($D/T>0.7$) and have two sections of blades at opposite angles. The objective is to pump the viscous fluid in one direction in the center core of the vessel and in opposite direction in the annular space. The outer blade of INTERMIG has two staggered sections designed for minimizing local form drag losses, which result in more distinct axial flow and lower power number. These impellers are used in multiples for liquid height to tank diameter ratio (H_1/T) of 1.0, eg, two for INTERMIG and three for MIG. Both impellers have been successfully used for low viscosity and multiphase systems also, but then D/T must be <0.7 and wall baffles are required.

Radial Flow Impellers (Fig. 5). Radial Flow impellers pump fluid in the outward direction toward the tank wall where, with the aid of baffles, the flow is split in upward and downward directions. Thus two recirculation regions are created, above and below the impeller. These impellers provide higher shear compared with axial flow impellers and are efficient for dispersion of mutually insoluble liquids and mixing of gas and liquid.

The basic radial flow impeller is flat blade turbine (FBT) with four or six vertical blades attached to a hub. A disk can be added to the FBT to fabricate a Rushton impeller. The vertical blades in these impellers can be curved to make back-swept impeller. The back-swept impeller has a power number $\sim$20% less than that with straight bladed impellers. Use of a disk in gas dispersion applications prevents bypassing of the gas along the shaft, and forces all gas feed to pass through the high shear region near the blade tip.

A cupped blade impeller, Scaba SRGT or Chemineer CD6 (also called Smith turbine), was developed to increase gas holding capacity over the Rushton turbine. The impeller blades are semicircular or parabolic in cross-section. This shape maintains good mixing at higher gas flow rates without flooding compared to the Rushton turbine.

Hydrofoil Impellers (Fig. 6). Hydrofoil impellers are axial flow impellers and provide more streamlined flow compared to impellers shown in Figure 4. They, however, provide lowest shear among turbine impellers, having three or four tapering twisted blades, which are cambered and sometimes manufactured with rounded leading edges. The blade angle at the tip is shallower than at the

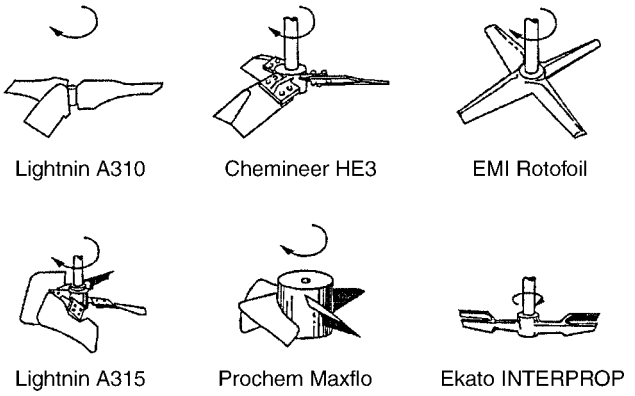

Fig. 6. Hydrofoil impellers.

hub, which creates a nearly constant pitch across the blade length. This produces a more uniform velocity across the entire discharge area. This blade shape results in a lower power number and higher flow for constant power consumption compared with a PBT. Lightnin A310, Chemineer HE3, and EMI Rotofoil are typical hydrofoil impellers with low power number and high pumping efficiency. Lightnin A315 and Prochem Maxflo are designed with high solidity ratio for gas dispersion and blending of non-Newtonian fluids. Solidity ratio is the ratio of projected blade area to the area swept by the impeller.

Ekato Interprop is a two-bladed hydrofoil with outside blade formed with two staggered sections. While the most common applications of hydrofoil impellers include blending of miscible liquids and suspension of solids, high solidity ratio hydrofoils are used for gas–liquid and liquid–liquid mixing systems.

High Shear Impellers (Fig. 7). High shear impellers are designed to be effective for fine dispersion of gas in liquid, emulsification, incorporation of powders etc. These dispersing impellers generate a low pumping rate, and therefore may need to be complemented with other axial flow or close-clearance impellers for homogeneity. A bar turbine is the lowest shear producer, a sawtooth impeller would be near the highest shear range, and Chemshear impeller provides intermediate shear. These mixers are typically operated at high speeds.

Rotor-Stator mixer consists of a high speed rotor placed in close proximity to a stator, both having uniquely designed slots. This mixer generates very high local

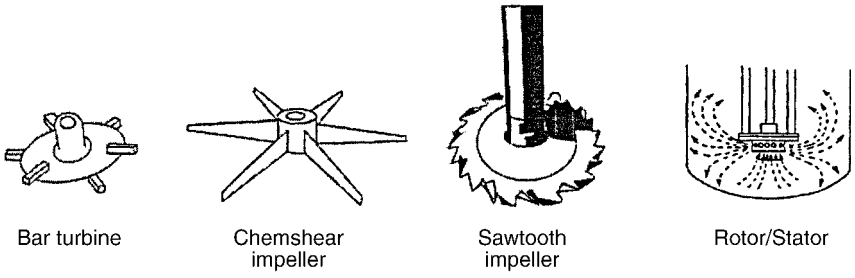

Fig. 7. High shear impellers.

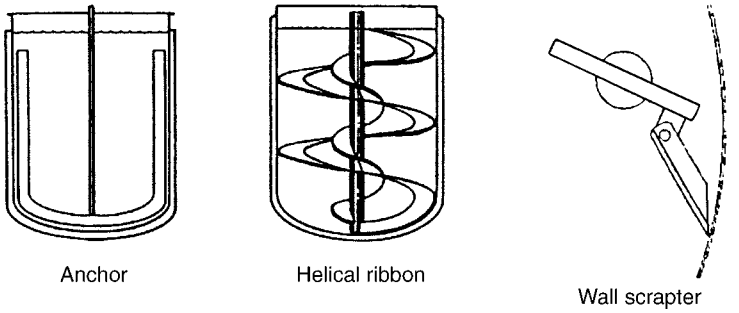

Fig. 8. Close-clearance impellers.

energy dissipation and shear rates and is commonly used for homogenization, dispersion, emulsification, grinding, dissolving etc. It can be used as an in-line mixer or in a batch tank where another recirculating impeller may be needed to provide bulk homogeneity.

Close-Clearance Impellers (Fig. 8). For mixing of high viscosity liquids, close-clearance impellers anchor and helical ribbon are most suitable. These impellers are large in size, almost the diameter of the vessel, and provide gentle macroscale blending of liquids at low shear. Anchors are sometimes complemented by single or multiple turbines installed on the shaft to provide additional shear in the bulk. In cosmetic applications these turbines may be required to operate at high speeds by an independent drive. Helical ribbons can have additional helixes including opposite pumping helix in the center. Both impellers can be equipped with wall scrapers on the blade tip (shown in Fig. 8) to maintain high heat-transfer coefficient in jacketed vessels.

2.3. Standards for Motor Power and Mixer Speeds. Mixer driver power and gear box speeds are generally available at standard levels. While the power levels of motors are universal, the speeds are dependent on the frequency of power supply. Table 2 gives standard motor powers and mixer speeds for North America where power supply is at 60-Hz frequency. Standard speeds will change where power supply frequency is different. These speeds are typical of gear drives with spiral-bevel and helical gears. Worm gears operate at other similar speeds such as 29, 35, 44, 58, 70, 88, 117, 146, 175, and 233 revolutions per minute (rpm). For higher speeds such as 1150, 1750, and 3500 rpm, direct drives are used typically in smaller size mixers.

Table 2. **Standard Motor Power and Mixer Speeds**

Motor power, HP						Mixer speed, rpm					
0.25	0.5	1	1.5	2	3	4	5	6	7.5	9	11
5	7.5	10	15	20	25	13.5	16.5	20	25	30	37
30	40	50	60	75	100	45	56	68	84	100	125
125	150	200	250	300	350	155	190	230	280	350	
400	500	600									

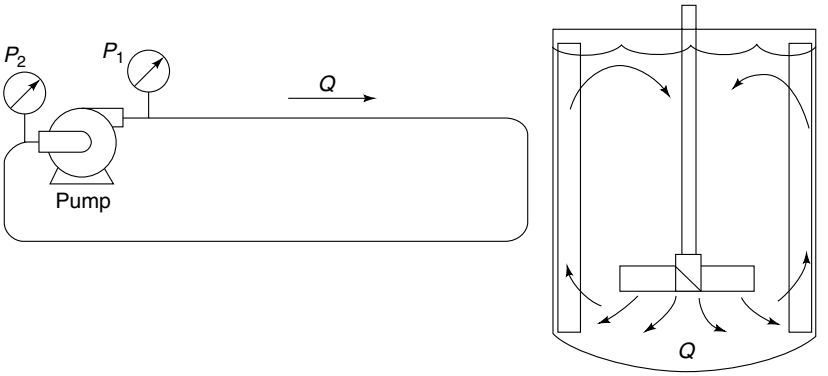

Fig. 9. Pump–mixer analogy.

3. Impeller Characeristics

3.1. Pumping, Velocity Head, and Power. Mechanical mixers can be compared with pumps (1) because they produce circulating capacity Q and velocity head H. The analogy between a pump and mixer can be appreciated by comparing a pumping loop with a mixing tank (Fig. 9).

Power input P to a pump is represented by

$$P = Q(P_1 - P_2)$$

The parameter Q in a mixer represents internal recirculation that is not confined and directed as in a pipe. The pressure drop in a mixer is analogous to velocity head H, which can also be considered degradation of kinetic energy. The parameter H is proportional to shear in mixing because head from kinetic energy generates shear through the jet or pulsating motion of the fluid. The parameter Q in a mixer is related to speed N and the impeller diameter D by

$$Q = N_q N D^3$$

The dimensionless pumping number N_q is a function of impeller type, the impeller/tank diameter ratio (D/T), and mixing Reynolds number $\mathrm{Re} = \rho N D^2/\mu$. Figure 10 shows the relationship (2) for a 45° pitched blade turbine (PBT). The values of N_q for several other impellers under turbulent conditions are given in Table 3.

The velocity head H in a pipe flow is related to liquid velocity v by $H = v^2/2g_c$, where g_c is acceleration due to gravity. The liquid velocity in a mixing tank is proportional to impeller tip speed πND. Therefore, H in a mixing tank is proportional to N^2D^2. The power consumed by a mixer can be obtained by multiplying Q and H and is given by

$$P = N_p \rho N^3 D^5 / g_c$$

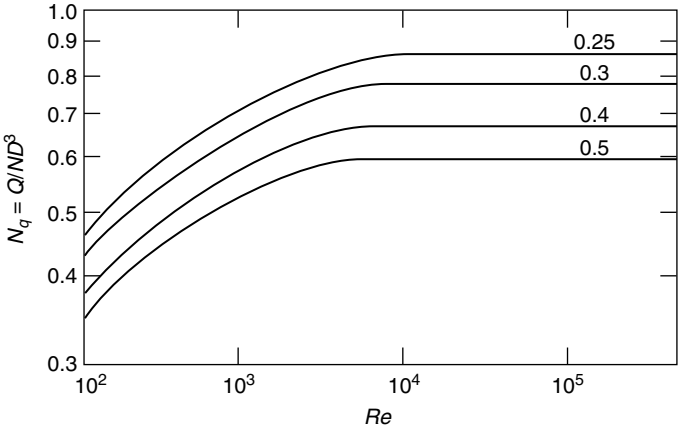

Fig. 10. Pumping numbers, N_q, versus mixing *Re* for a pitched blade turbine. The numbers on the curves represent the ratio D/T.

Table 3. **Pumping Number N_q, for Various Impellers under Turbulent Conditions**

Impeller type	Propeller	Hydrofoil	Pfaudler	FBT	Rushton	Chemineer CD6
N_q	0.4–0.6	0.55–0.73	0.3	0.7	0.72	0.76

The dimensionless power number N_p depends on impeller type and mixing *Re*. Figure 11 shows this relationship for six commonly used impellers. Similar plots for other impellers can be found in the literature. The functionality between N_p and *Re* can be described as $N_p \propto Re^{-1}$ in laminar regime ($Re < 10$) and depends on liquid viscosity μ; N_p in turbulent regime ($Re > 10{,}000$) is constant and independent of μ.

Other parameters, such as blade width W, number of blades n, and blade angle α, also affect the power number as follows:

For 6-bladed Rushton	$N_p\alpha\ (W/D)^{1.45}$
For 4-bladed PBT	$N_p\alpha\ (W/D)^{0.65}$
For 3–6 blades	$N_p\alpha\ (n/D)^{0.8}$
For 6–l2 blades	$N_p\alpha\ (n/D)^{0.7}$
For PBT	$N_p\alpha\ (\sin\alpha)^{2.6}$

The number of wall baffles N_b and their width B also have a significant effect on N_p. As N_bB increases, N_p increases (Fig. 12**a**) up to the N_p of the conventional configuration with four baffles having width equal to $T/10$. At higher N_bB the power number is constant at a level that depends on D/T. For multiple impellers, N_p increases as spacing S_i between the impellers is increased (Fig. 12**b**). For $S_i/D > 1$, the power consumption reaches a plateau. This effect of S_i

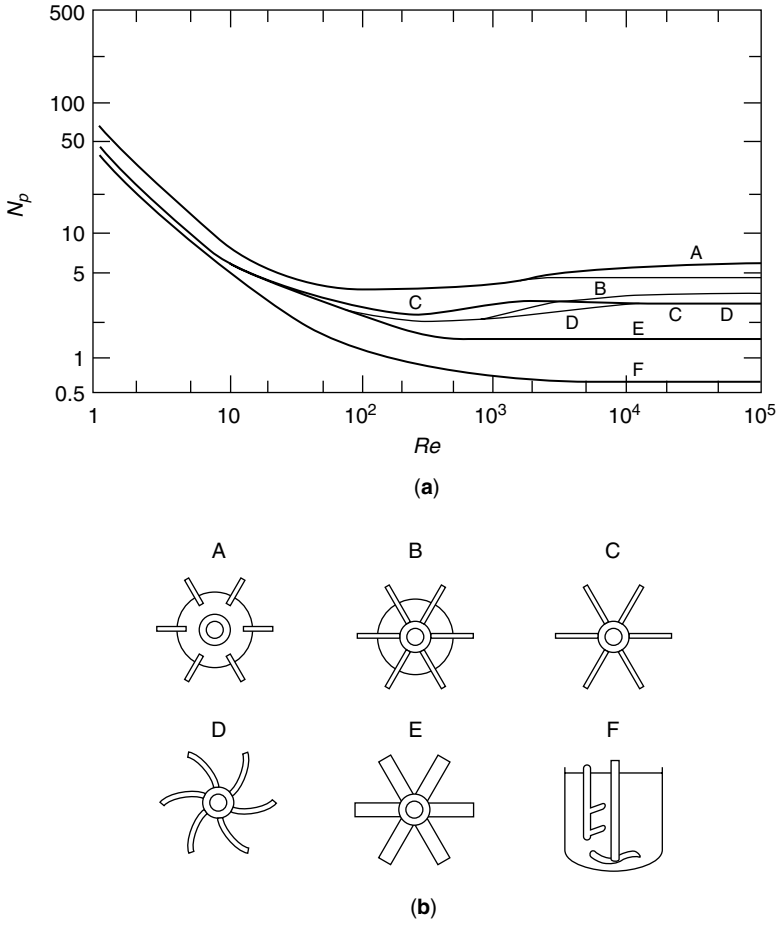

Fig. 11. (**a**) Power number versus Reynolds number; (**b**) Impellers represented as A-Rushton, blade width = $D/5$, B-Rushton, blade width = $D/8$, C-FBT, D-Curved blade turbine, E-PBT, F-Pfaudler retreat curve.

on N_p is different for PBT and a flat blade turbine (FBT), the latter showing a maximum at S_i/D=0.3. Also, in the range of S_i/D between 0.1 and 1.0, the N_p of two FBTs is more than twice that of a single FBT.

The effect of impeller elevation C on power number is small for radial flow impellers, but can be high for PBT. As shown in Figure 13, N_p decreases as C/D increases for PBT. These differences are due to different flow patterns, axial with PBT and radial with FBT and Rushton.

Power numbers for several other commonly used impellers under turbulent conditions are given in Table 4.

The power number of side entering propeller mixer depends on the pitch and mixing Reynolds number. The propeller pitch is defined as the distance traversed by the propeller in one revolution divided by the diameter. As shown in Figure 14, N_p of propeller increases as pitch is increased, especially at high Re.

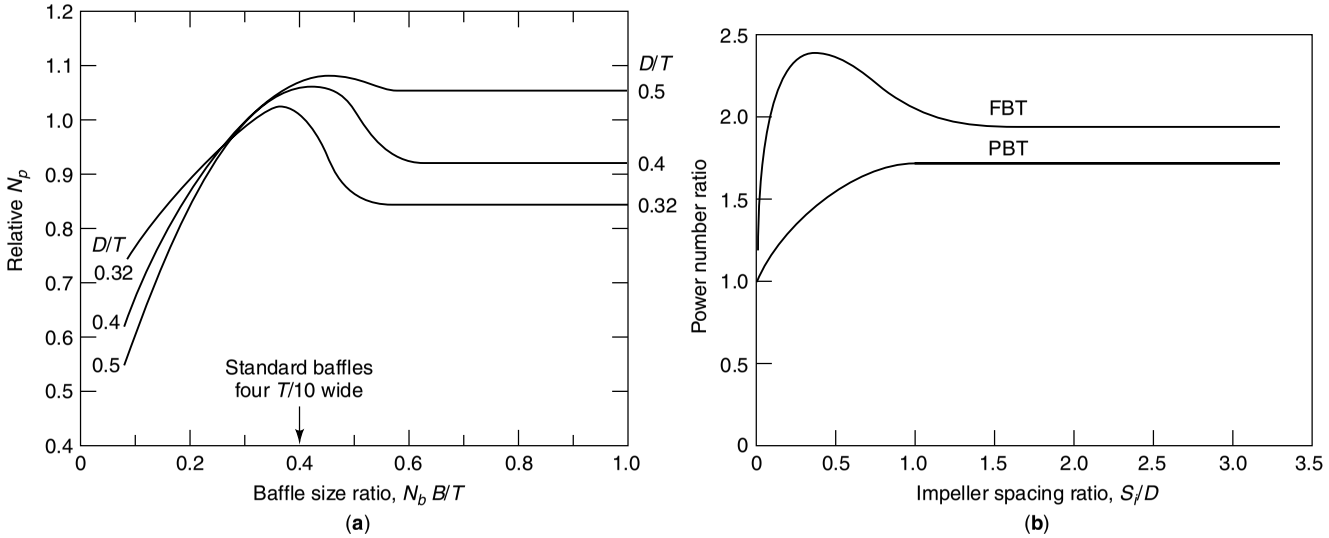

Fig. 12. (**a**) Effect of baffling and D/T on power number N_p relative to N_p for standard configuration; and (**b**) effect of dual impeller spacing on power number ratio of two impellers to one impeller.

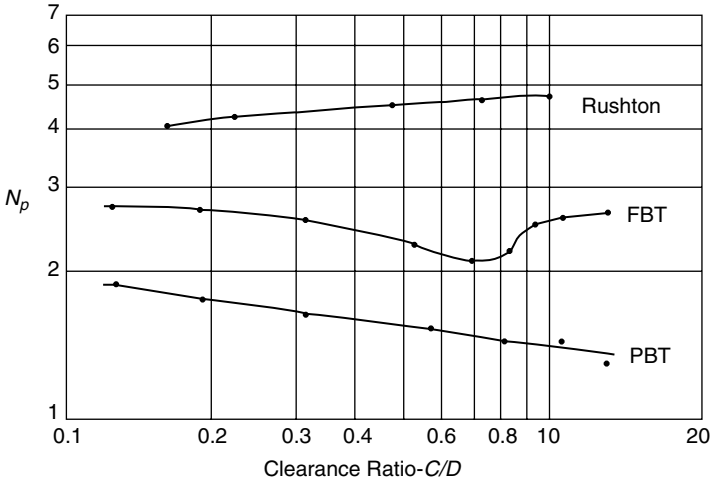

Fig. 13. Effect of impeller clearance on power number.

The power number of anchor agitator depends on wall clearance and Reynolds number as shown in Figure 15. The parameter N_p of round bladed anchor is slightly lower than that of flat bladed anchor. The effect of wall spacing (e) and height of anchor arm (h) on N_p for anchor can be described by

$$N_p \ \alpha (e/T)^{-0.5} \qquad \text{for} \qquad Re < 30$$
$$N_p \ \alpha (e/T)^{-0.25} \qquad \text{for} \qquad 30 < Re < 1000$$
$$N_p \ \alpha \{0.89(h/D) + 0.11\}$$

The power number for helical ribbon mixer depends on the Re, wall clearance e, height h, pitch of helix p, blade width w, and number of helical flights n.

$$N_p = \frac{150}{Re}\frac{h}{D}\sqrt{\frac{n}{\frac{p}{D}\left(\frac{e}{w}\right)^{0.67}}}$$

Depending on the process needs, the combination of pumping and shear can be changed by merely changing the impeller diameter and the mixer speed. A

Table 4. **Power Numbers of Various Impellers Under Turbulent Conditions Using Four Standard Size Wall Baffles**

Imeller Type	N_p
Ekato mig - 3 Impellers $D/T = 0.7$	0.55
Ekato INTERMIG - 2 Impellers $D/T = 0.7$	0.61
Sawtooth Impeller	0.2
Chemineer CD6	3.1
Lightnin A310	0.3
Chemineer HE3	0.3

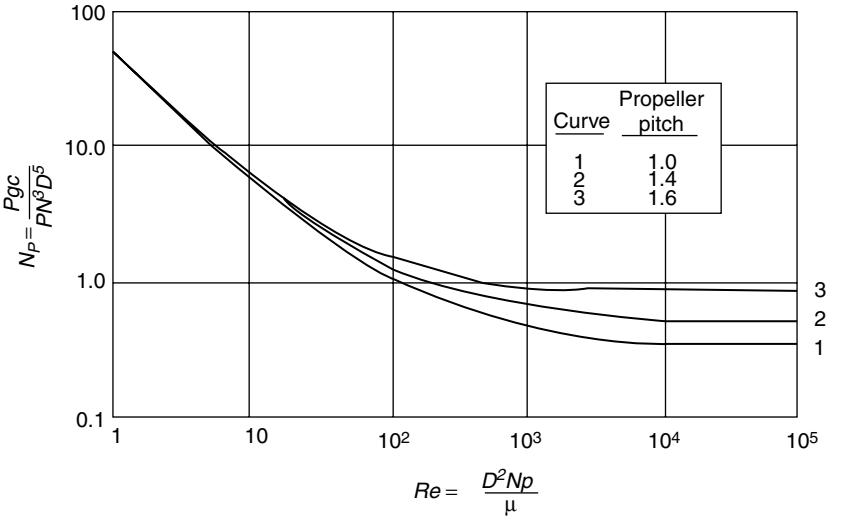

Fig. 14. Power number of propeller versus *Re*.

larger diameter impeller at slow speed would provide high pumping action necessary for systems such as blending and solids suspension. On the other hand, a small diameter impeller and high mixer speed would be more suited for high shear systems where mass transfer is important. At constant power input the ratio of pumping capacity to head is related to impeller diameter as

$$Q/H \propto D^{8/3}$$

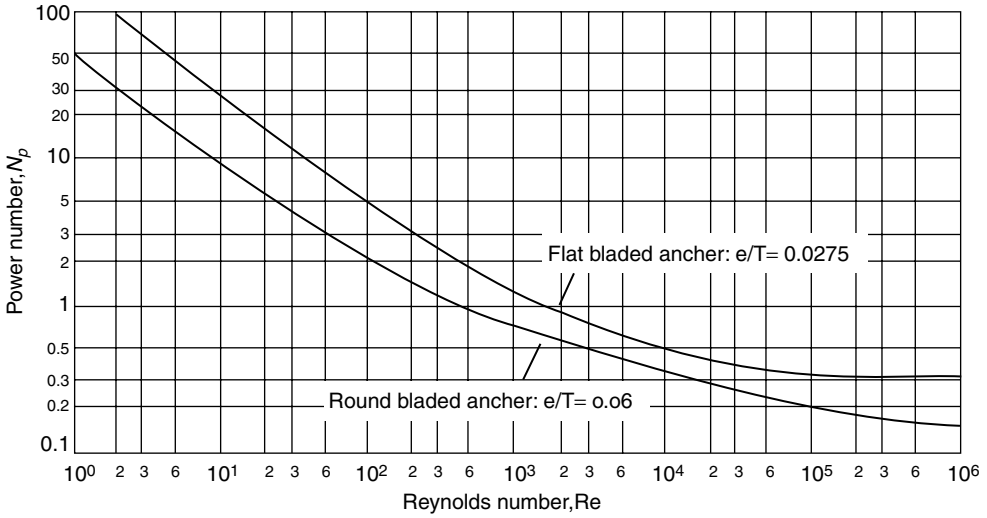

Fig. 15. Power number plots for anchor agitators at two wall clearances.

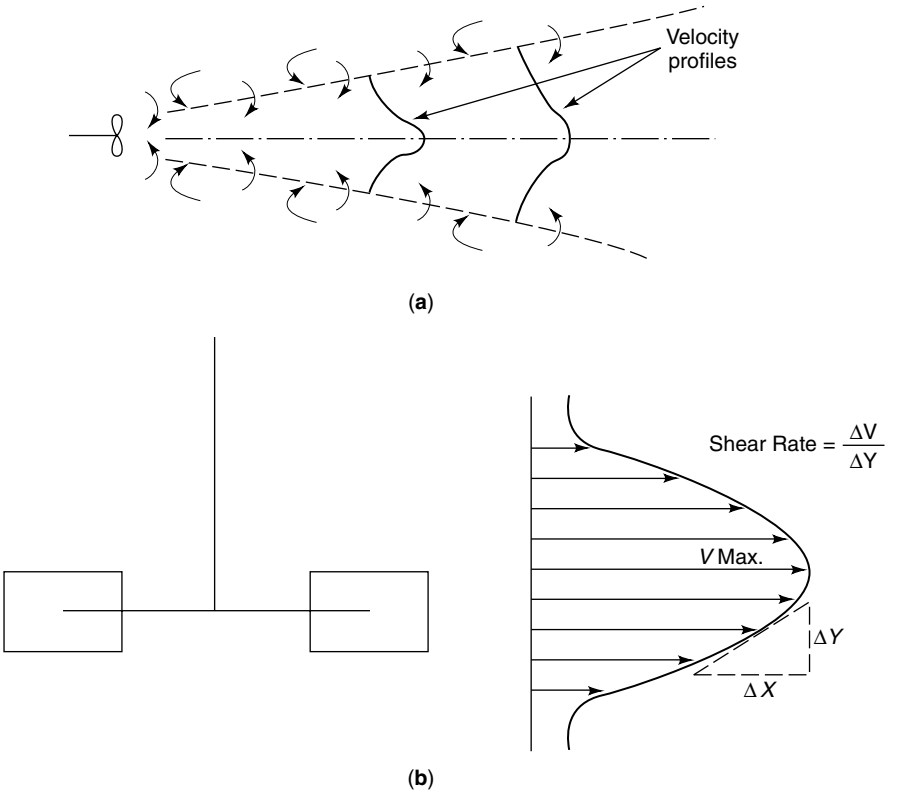

Fig. 16. (**a**) Liquid entrainment and velocity profiles in propeller jet. (**b**) Vertical velocity profile near impeller blade tip where the shear rate $= \Delta V/\Delta Y$.

Shear Rate–Shear Stress. Whenever there is relative motion of liquid layers, shearing forces exist that are related to flow velocities. These forces, represented by shear stress, carry out the mixing process and are responsible for producing fluid intermixing, dispersing gas bubbles, and stretching or breaking liquid drops. The shear stress is a function of shear rate defined by the velocity gradients $\Delta V/\Delta Y$, impeller blade pressure drop, turbulence level, and viscosity.

$$\text{Shear stress} = \mu \times \text{shear rate}$$

Shear rate represented by velocity gradients can be caused by either entraining liquid with a propeller jet (Fig. 16**a**) or by creating velocity profiles with rotating impellers (Fig. 16**b**). Velocity profiles in the propeller jet are proportional to the jet velocity at the blades. The total flow increases by entrainment of the fluid surrounding the jet, whereas the velocity decreases as the jet expands.

Obviously, shear rate in different parts of a mixing tank is different, and therefore there are several definitions of shear rate: (*1*) for average shear rate in the impeller region, $\propto N$, the proportionality constant varies between 8 and

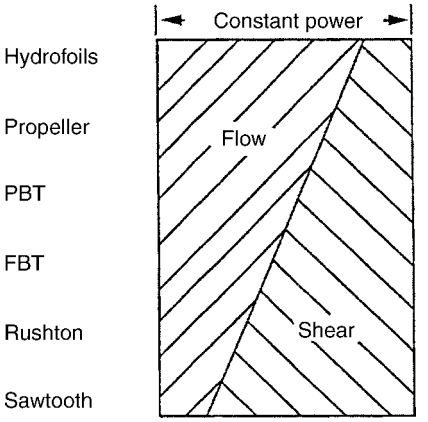

Fig. 17. Order of impellers by pumping and shear.

14 for all impeller types; (*2*) maximum shear rate, $\propto$ tip speed (πND), occurs near the blade tip; (*3*) average shear rate in the entire tank is an order of magnitude less than case *1*; and (*4*) minimum shear rate is $\sim$25% of case *3*.

In turbulent mixing, the liquid velocity at any point u can be considered the sum of an average velocity $\bar{u}$; and a fluctuating (with time) velocity u':

$$u = \bar{u} + u'$$

Because u' can be positive or negative, its impact on mixing is best quantified by calculating the (root mean square) rms fluctuation. The rms velocity is obtained by squaring the fluctuation, time averaging, and then taking the square root. Turbulent intensity is defined as ratio of rms velocity to average velocity. Typically, turbulent intensity ranges from 0.5 to 0.7 near the impeller tip, to 0.05 to 0.15 in other parts of the tank.

Turbine impellers can be represented in the order of relative pumping and shear as shown in Figure 17. Hydrofoils are near the high end of flow range but low end of shear range, while Rushton and Sawtooth impellers are at opposite ends. Other impellers produce intermediate flow and shear.

Macromixing, Mesomixing and Micromixing. Mixing in an agitated tank is considered to occur at three levels; macromixing, mesomixing and micromixing.

Macromixing is driven by the large scale of fluid motion and is established by the mean convective flow pattern. It is sufficient for certain mixing duties such as coarse scale blending of miscible liquids for concentration homogeneity via mean velocities and turbulent dispersion.

Mesomixing occurs at a relatively smaller scale than the bulk circulation. It is most frequently evident in the region of feed nozzles and results in a reduction of the scale of segregation between feed and bulk fluids.

Micromixing occurs by turbulent diffusion and causes complete intermingling of molecules. It is necessary for fast reacting systems or when enhancement of mass transfer is desired. In a turbulent field, eddies are generated in

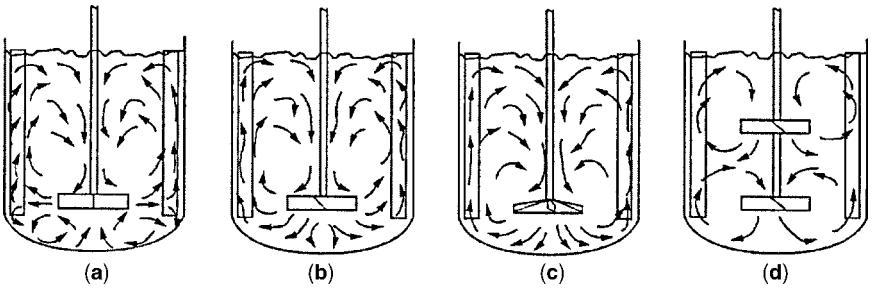

Fig. 18. Flow patterns with different impeller types, sizes, and liquid viscosity: (**a**) FBT; (**b**) PBT; (**c**) hydrofoil; (**d**) two PBTs.

varying sizes having a maximum scale of the size of the equipment to a minimum length scale defined as Kolmogoroff microscale η:

$$\eta = [\nu^3/\epsilon]^{1/4}$$

where ν is kinematic viscosity of solution and ϵ is energy dissipation rate per unit mass of fluid. Mixing energy is transferred from the largest eddies to the smallest eddies until it is eventually dissipated through friction in viscous and turbulent shear stresses and finally appears as heat in the system.

Flow Patterns. As described earlier, turbine impellers are classified based on two types of flow patterns radial flow and axial flow (3). Radial flow impellers produce two circulating loops, one below and one above the impeller (Fig. 18**a**). Mixing occurs between the two loops, but less intensely than within each loop. Axial flow impellers (PBT), on the other hand, produce a flow pattern (Fig. 18**b**) involving full tank volume as a single stage. True axial flow is usually created with hydrofoil impellers (Fig. 18**c**), which provide a confined flow similar to that created in a draft tube. Multiple impellers are used when liquid depth-to-tank diameter ratio is >1. In that case, more circulation loops are formed, eg, two loops with PBT (Fig. 18**d**). These differences in flow patterns cause variations in shear rate distributions in the tank so that the process result is highly impacted by the impeller flow patterns. The flow patterns within a given impeller are also altered by parameters such as impeller diameter and liquid viscosity. For example, the flow pattern with a PBT becomes closer to radial as the impeller diameter is increased or liquid viscosity is increased.

Wall Baffles. Because rotating impellers mainly create tangential flows in transitional and turbulent flow regimes, wall baffles are needed to transform them to vertical flows, and hence top-to-bottom liquid mixing. These baffles located along the tank wall are necessary for eliminating a swirl and cavitation. The standard baffle configuration consists of four vertical plates having width equal to 8–10% of tank diameter. Narrower baffles are sometimes used for high viscosity systems, buoyant particle entrainment (width = 2% of T), or when a small vortex is desired. A small spacing between baffles and the tank wall (1.5% of T) is allowed to minimize dead zones particularly in solid–liquid systems. The presence of wall baffles, however, causes an increase in power consumption (Fig. 12**a**), but generally enhances the process result. In square and

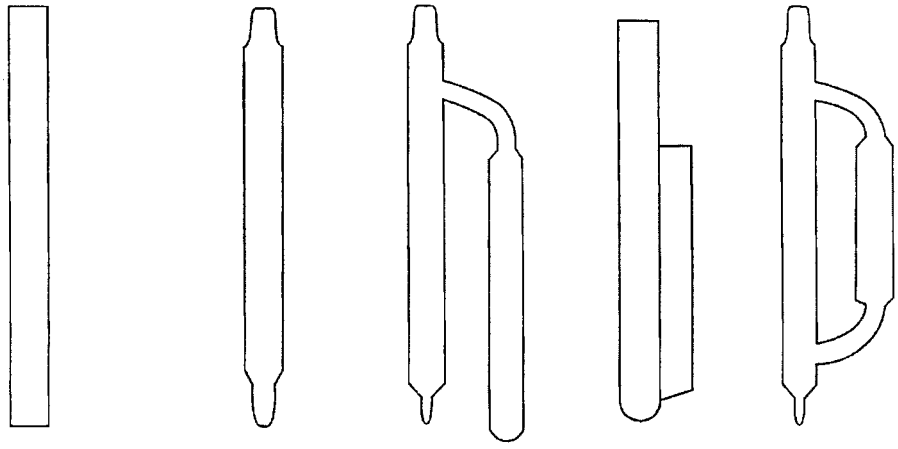

Fig. 19. Baffle types.

rectangular shaped tanks, the corners break up the tangential flow pattern thus providing the baffling effect, and wall baffles may not be needed.

For glass lined vessels, different types of baffles, shown in Figure 19, are used for convenient installation through flanges on the vessel top. These include a fin, h style and D style. For mixing of floating solids slurries a single wide surface baffle is used to create a small precessing vortex.

Dimensionless Numbers. With impeller diameter D as length scale and mixer speed N as timescale, common dimensionless numbers encountered in mixing depend on several controlling phenomena (Table 5). These quantities are useful in characterizing hydrodynamics in mixing tanks and when scaling up mixing systems.

Where Q_g is gas sparging rate, h is process side heat transfer coefficient, k is thermal conductivity of fluid, C_p is specific heat of fluid, $\Delta\rho$ is thermal density difference between two fluids, ρ is fluid density, σ is interfacial tension and σ_1 is normal stress.

Table 5. **Dimensionless Numbers Used in Mixing**

Number	Formula	Important for
flow, *Fl*	Q_g/ND^3	gas dispersion
Froude, *Fr*	N^2D/g	free surface or vortexing
Nusselt, *Nu*	hT/k	heat transfer
power, N_p	$P/\rho N^3D^5$	power consumption
Prandtl, *Pr*	$C_p\mu/k$	heat transfer
pumping, N_q	Q/ND^3	blending
Reynolds, *Re*	$\rho ND^2/\mu$	laminar or turbulent flow
Richardson, *Ri*	$g\Delta\rho l/\rho\mu^2$	blending
viscosity ratio, V_i	μ_1/μ_2	viscosity differences
Weber, *We*	$\rho N^2D^3/\sigma$	emulsification
Weissenberg, *Wi*	$\sigma_1/N\mu$	viscoelastic effects

Scale-Up Principles. The main objective of scale-up is to achieve the same quality of mixing in a commercial size mixing tank as in a laboratory test tank, or at least have an understanding of the differences expected in the commercial process result. Unfortunately, it is not possible to maintain the same combination of flow and shear distributions in commercial mixers as in small-scale tanks. Several scale-up methods have been developed depending on the process type and mixing requirements, but all methods emphasize geometric similarity. Otherwise correction factors are required that lead to high uncertainties in the prediction of the process result. Geometric similarity refers to maintaining the same impeller type, and relative dimensions of impeller, impeller elevation, liquid height, and baffles.

The most commonly used scale-up criterion uses constant power per unit volume (P/V), which is usually conservative. Depending on the process requirement, P/V should be increased or decreased with increase in volume according to $P/V = \text{constant } V^y$. The scale-up exponent y can be negative or positive and should be determined either through pilot plant testing or from recommended values in Figure 20. With constant P/V scale-up, the average shear decreases while the maximum shear rate increases. The effect of these shear rate changes on the process result must be established experimentally. Scale-up based on constant torque per unit volume (T_q/V) is considered by some engineers to be more desirable because it is related to the magnitudes of the fluid velocities. Torque is related to the mixer power by $T_q = P/2\pi N$. Similar to P/V scale-up, T_q/V is changed proportional to the volume to an exponent that can be obtained either experimentally or from standard values.

When choosing the scale-up method, changes in other flow/power parameters and their impact on the process result must be considered. Table 6 shows how these important parameters change on scale-up to 1000 times the

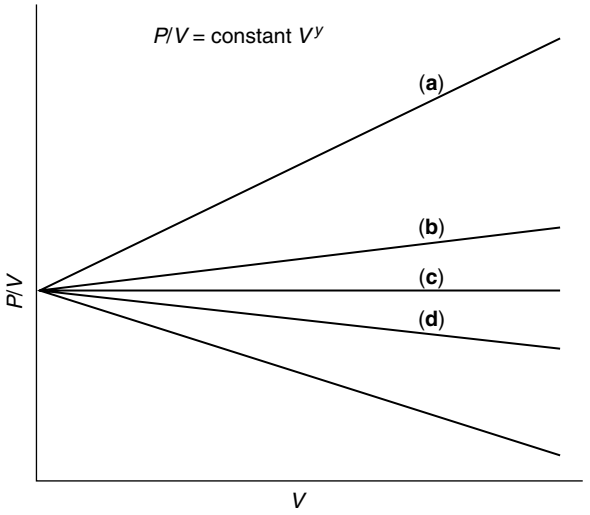

Fig. 20. Log–log plot scale-up by power per unit volume where for (**a**) constant blend time, $y = 2/3$; (**b**) same vortex, $y = 1/6$ (**c**) dispersion, $y = 0$; (**d**) solids suspension, $y = -1/12$; and (**e**) constant flow velocity, $y = -1/3$.

Table 6. **Changes in Mixing Parameters on Scale-Up by a Factor of 10 in Diameter and 1000 in Volume for Geometrically Similar Systems**

$N,Q/V$	Q	*Tip speed*	*Re*	T_Q/V	*We*	P/V	P
1	1000	10	100	100	1000	100	10^3
0.1	10	**1**	10	**1**	10	0.1	100
0.22	220	2.2	21.5	4.8	48.4	**1**	1000

volume. For turbulent conditions for example, scale-up based on same tip speed maintains the T_q/V but decreases P/V by 90%. T_q/V is almost always increased on scale-up. Scale-up based on the same P/V means a reduction in mixer speed by 78%, which also translates to an increase in blend time by a factor of 4.6. This is acceptable in most applications except in very fast reacting systems which are scaled-up based on constant mixer speed. It should be noted that for constant P/V scale-up, Reynolds number increases by a factor of 21.5. This changes the flow regime and may affect the mixing quality. Most practical scale-up methods are between equal P/V and equal T_q/V.

When the process controlling mixing parameter is unknown, laboratory and pilot-plant experiments should be carried out at different mixer speeds. Variability of the desired process result with P can be a good indicator of the controlling regime. For example, no effect with increasing P indicates kinetic regime in a homogeneous reaction. Increase in the process result proportional to P^x $(0.5 < x < 1.0)$ means mass-transfer control. For suspension of solids with high settling velocity, constant P/V is required in scale-up. However, constant tip speed suffices for slow settling solids. The criterion valid for dispersion processes involving liquid–liquid and gas–liquid systems is constant P/V. This method maintains the same interfacial area per unit volume, hence the same mass-transfer rate. However, considerable deviation from constant P/V is needed if other factors such as coalescence, velocities, static pressure, etc, affect the process result.

4. Blending of Miscible Liquids

Mutually soluble liquids are blended to provide a desired degree of uniformity in an acceptable mixing time. Agitator effects are critical particularly in commercial operations when both product quality and production rates are important. The mechanism of blending differs significantly for low-to-medium viscosity liquids and high viscosity liquids. Therefore mixing system designs and mixing time correlations need to be discussed sepratately for the two liquid types. In addition, rheological properties can have large impact on mixing time and methodology for its estimation will also be described.

4.1. Blending of Low-to-Medium Viscosity Liquids. *Newtonian Liquids.* In agitated tanks, mixing time and pumping rate for a given impeller are related. This relationship can be different with different impeller types. For designing axial flow turbines there are three useful methods for determining blend time, tank turnover, bulk fluid velocity, and dimensionless blend time.

1. *Tank turnovers* method is based on impeller pumping rate and liquid volume. Pumping rate of an impeller can be estimated from impeller diameter and mixer speed, and the pumping number N_q for a PBT can be obtained from Figure 10. Turnover rate in a mixing tank is obtained by dividing pumping rate Q by the tank volume V. Blend time can then be estimated by defining the number of turnovers needed for the process result. It is recommended that the turnover requirements be defined through laboratory testing on the basis of a specific process result. The approximate numbers of turnovers required for different liquid viscosity ranges are as follows:

liquid viscosity, mPa s	Up to 100	100–1000	1000–5000	>5000
number of turnovers	3	10	50	>100

2. *The bulk fluid velocity* method relates a blending quality ChemScale number C_n to a qualitative description of mixing (Table 7). The value of C_n is equal to one-sixth of the bulk fluid velocity defined by pumping rate divided by cross-sectional area of the tank (4). An appropriate ChemScale must be chosen based on physical properties of the liquids to be blended and level of mixing desired.
3. *Dimensionless blend time* method uses correlations developed based on experimental data with a variety of impellers and tank configurations. This dimensionless blend time is defined as $N\theta$, where N is mixer speed and θ is blend time for 95% homogeneity.

   For turbulent flow (Re >10,000) regime the value of $N\theta$ is found to be constant for a given impeller type and diameter, vessel diameter and liquid height. The following correlation has been developed with data from a variety of axial flow, radial flow and hydrofoil impellers, and different impeller and tank configurations.

$$N\theta = 5.2\ T^{1.2}H^{0.5}/D^2N_p^{1/3}$$

For a tank with height equal to diameter,

$$N\theta = 5.2/N_p^{1/3}(D/T)^2$$

Table 7. **Mixing Quality Descriptions for ChemScale Numbers, C_n**

C_n	*Specific gravity difference*, $\Delta\rho$	*Viscosity ratio*, μ_1/μ_2	*Solids suspension for <2% slurries*	*Surface motion*
2	<0.1	<100	no	fluid surface flat but moving
6	<0.6	<10,000	Settling rates 0.6–1.2 m/min	rippling surface at low μ
10	<1.0	<100,000	Settling rates 1.2–1.8 m/min	surging surface at low μ

This equation can be transformed to dimensionless form as

$$Fo = 5.2/ReN_p^{1/3}$$

where Fo= Fourier number =$\mu\ \theta/\rho T^2$
Through these relationships it can be shown that

- All impellers of same size provide same blend time at same P/V.
- A larger impeller will provide shorter blend time for same P/V.
- Blend time is independent of liquid physical properties for turbulent conditions.
- With constant P/V scale-up, blend time increases by $T^{2/3}$.

For transitional flow ($200<Re<10{,}000$), the dimensionless blend time is found to be inversely proportional to Re and the proportionalty constant depends on impeller type and impeller to tank diameter ratio.

$$N\theta = \text{constant}/Re = 33,500/Re(D/T)^2N_p^{2/3}$$

This equation in dimensionless numbers can be written as

$$Fo = 33,500/Re^2N_p^{2/3}$$

These correlations indicate that

- All impellers of same size provide same blend time at same P/V.
- A larger impeller will provide shorter blend time for same P/V.
- Blend time is proportional to μ/ρ for transitional flow.
- With constant P/V scale-up, blend time decreases by $T^{-2/3}$.

Non-Newtonian Shear Thining Liquids. Shear thining liquids are characterized by power law correlation between shear stress τ and shear rate γ

$$\tau = K\dot{\gamma}^n \quad \text{where } n < 1.0$$

therefore apparent viscosity μ_a can be calculated from

$$\mu_a = \tau/\dot{\gamma}\ = K\dot{\gamma}^{n-1}$$

Due to shear rate dependency, apparent viscosity in different parts of the vessel is different. For example, μ_a is lower in the high shear zone near the impeller blade compared to a lower shear region near the liquid surface. A wall shear stress model, described in the *Handbook of Mixing* (Ref. 5), can be used to estimate the blend time. However, for a first pass estimate of blend time, one can use the correlations for Newtonian liquids and using apparent viscosity.

When a liquid-filled tank is stratified with denser liquid at the bottom, higher mixing energy is needed to cause homogeneity. The time to break up stratification depends on the rate of erosion of the interface. This interface rises to the liquid surface at a rate based on horizontal velocities at the interface. The entrainment velocity is correlated with the Richardson number, Ri, which is the ratio of buoyant to inertial forces. When $Ri<7$ the rise of the interface is fast enough to ignore the time taken for breakup of the layers. Therefore, the blend time for 95% homogeneity θ_{95} mainly depends on the time taken for a desired liquid homogeneity as estimated above. If, however, mixing quality better than 95% is desired, the blend time can be estimated using a variance decay model for fractional homogeneity x:

$$(1-x) = e^{-k\theta}$$

By using a known reference blend time for 95% homogeneity, blend time for better homogeneity can be obtained by

$$\theta_x = -\theta_{95} \ln(1-x)/3$$

4.2. Viscous Liquid Blending in Laminar Regime. Viscous liquids are classified based on their rheological behavior characterized by the relationship of shear stress with shear rate. For Newtonian liquids, the viscosity represented by the ratio of shear stress to shear rate is independent of shear rate, whereas non-Newtonian liquid viscosity changes with shear rate. Non-Newtonian liquids are further divided into three categories: (*1*) time-independent, (*2*) time-dependent, and (*3*) viscoelastic. A detailed discussion of these rheologically complex liquids is given elsewhere (see RHEOLOGY AND RHEOLOGICIAL MEASUREMENTS).

As liquid viscosity is increased, the discharge stream velocity from an impeller is more rapidly dissipated by liquid friction. As a result, the flow pattern flattens out and axial flow impellers generate radial flows. This change significantly affects blending quality. For example, if an axial flow impeller circulates low viscosity liquid to a height of four impeller diameters above and below, it circulates a 50,000-mPa s liquid to only $D/2$ height above and below. This indicates good mixing in a small volume around the impeller while little interchange of material occurs outside of this volume. Under these conditions mixing can best be achieved with proximity or close-clearance impellers such as anchor and helical ribbon (see Fig. 8)

Among the close-clearance impellers, anchors are effective for liquid viscosities in the range of 5000–50,000 mPa s. Above 50,000 mPa s, pumping capacity of the anchor declines and the impeller simply "slips" in the liquid. Helical ribbon impeller is more effective at these viscosity levels, because they provide better top-to-bottom liquid turnover. They are sometimes used with two helixes, outer one with size 90–95% of vessel diameter and an inner one of small diameter, each pumping in opposite directions. The pitch of helix, defined as height of one 360° turn, is usually equal to impeller diameter; and the width is typically 10% of impeller diameter. Higher pitch reduces top-to-bottom mixing, whereas lower pitch causes excess friction and energy consumption.

For a given helical ribbon impeller; the dimensionless blend time, $N\theta$, is constant for high viscosity liquids under laminar flow conditions. This means that the dimensionless blend time is independent of liquid viscosity. This constant, however, is a function of helical ribbon pitch and blade width as described in the following equations.

$$N_\theta = 8.96 \times 10^5 \, K_p^{-1.69}$$

where

$$K_p = 173.1(p/D)^{-0.72}(w/D)^{0.14}$$

4.3. Blending of Viscoelastic Liquids. Both turbine and close-clearance impellers are used depending on liquid viscosity range. As the impeller rotates in these liquids, normal stresses are created in addition to the usual tangential stresses, thereby causing the liquid to climb up the shaft called Weissenberg effect (shown in Fig. 21). This results in longer mixing times and higher power number in the laminar regime.

4.4. Feedpipe Backmixing. Backmixing of fluid into the feedpipe can result in lower yields of the desired product in a system with fast competitive–consecutive reactions. This is because some reactions can occur in unmixed conditions in the feedpipe where the reacting species may be in nonstoichiometric ratios. Therefore, it is important to design the feed injector nozzles to provide minimum jet velocity v_f to prevent backmixing into the feedpipe. This minimum feed jet velocity depends on impeller type, mixer speed, and the feedpipe location. For a given impeller type and feedpipe location, the ratio of minimum v_f to tip speed v_t is nearly constant. The minimum values of this ratio v_f/v_t for preventing feedpipe backmixing are 1.9 for Rushton with radial feed, 0.25 for Rushton with feed above impeller, 0.1 for HE-3 with radial feed, and 0.15 for HE-3 with feed above impeller.

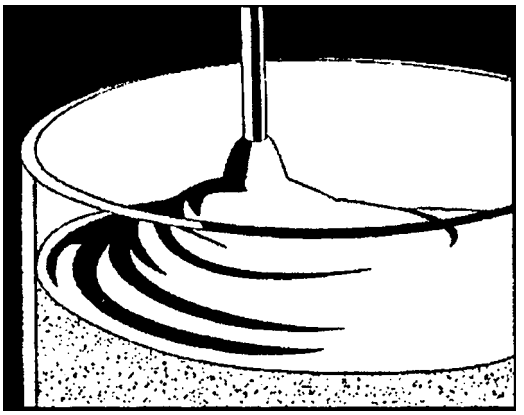

Fig. 21. Weissenberg effect with mixing of viscoelastic liquid.

5. Suspension of Solids

Solids are suspended in liquid-filled agitated tanks for the purpose of dissolution, accelerating chemical reactions or preparing a homogeneous slurry. Typical industrial applications include catalyst suspension, rubber particle slurrying, TiO_2 slurry for paper coatings (qv), activated carbon suspension in water treatment, or slurrying in leaching of metals. In most applications it is important to select a suitable mixer type that can be designed to provide the desired process result at minimum energy consumption. This requires understanding of the mixing mechanism of solids suspension and possibly laboratory testing to develop design guidelines. The critical mixing parameters depend on whether the particles sink or float under unmixed conditions, and therefore are discussed separately for the two types of solids.

5.1. Sinking Solids. Lifting and distribution of solids heavier than the liquid is accomplished by inducing necessary flow patterns by expending mechanical energy. This energy, supplied by a rotating impeller, is dissipated in turbulent eddies having a variety of sizes. The largest velocity scale of turbulent eddies is on the order of maximum tip speed, whereas the largest length scale of eddies is on the order of the impeller size. According to the Kolmogoroff principle of isotropic turbulence, small eddies are 30–100 μm in size. Because most solids of industrial importance are 1 mm or larger, small eddies are ineffective in suspending them; only large-scale liquid motion is responsible for their suspension. When the velocity scale of large eddies is higher than the free settling velocity of particles, entrainment occurs. For particle suspension from the rest position, this free settling velocity must be overcome. The energy requirement for maintaining a suspension is, however, much less.

Measurement of single particle settling velocity in a turbulent field is not easy. However, it is known to be a function of free settling velocity u_t, which for spherical particles can be estimated from the following:

$$u_t = \sqrt{\frac{4gD_p\Delta\rho}{3\rho C_D}}$$

Where D_p is particle diameter, ρ is liquid density and Δρ is density difference between solids and liquid. The drag coefficient C_D has different functionalities with particle Reynolds number Re_p ($=D_p u_t \rho_l/\mu$) in three different regimes (Fig. 22), which results in the following expressions for particle settling velocity (1).

Region	Stokes	Intermediate	Newton
Re_p	<0.3	$0.3–10^3$	$10^3–10^5$
u_t	$\frac{gD_p^2\Delta\rho}{18\,\mu}$	$\frac{0.15g^{0.7}D_p^{1.14}\Delta\rho^{0.7}}{\rho^{0.3}\mu^{0.4}}$	$1.74\sqrt{\frac{gD_p\Delta\rho}{\rho}}$

Quite often the settling velocity is modified by the presence of a large number of particles. This hindered settling velocity is a function of solids

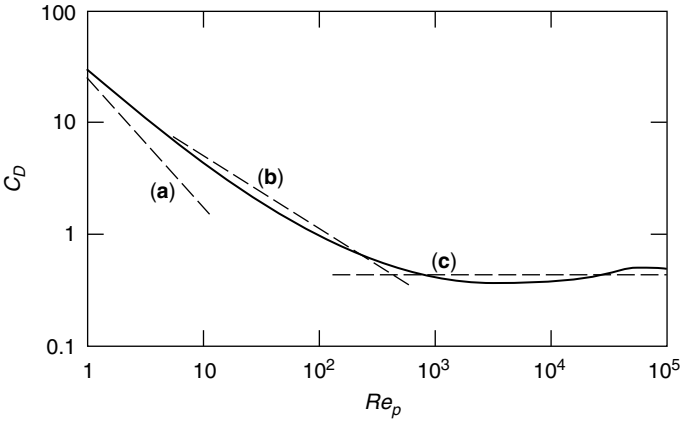

Fig. 22. Drag coefficient C_D for terminal settling velocity correlation (single particle) where **a**, represent Stokes law; **b**, intermediate law; and **c**, Newton's law (1).

concentration and should be measured experimentally or estimated from literature correlations (1).

In solids suspension applications it is desirable to have at least movement of particles on the tank floor, although this type of mixing is rarely sufficient. This condition is called partial suspension, as shown in Figure 23, and settled fillets of solids can be expected on the tank floor. For most situations off-bottom suspension is necessary, ie, all particles are suspended even though they may temporarily settle before being lifted again. Some processes require complete slurry uniformity or full suspension, which for practical purposes is achievable only up to 95–98% of liquid height. Between off-bottom suspension and full suspension, there are several mixing quality levels defined by the ratio of solids concentration near the top to bulk concentration. In mass-transfer operations, as mixer power is increased, the mass-transfer coefficient, k_L, increases rapidly up to the

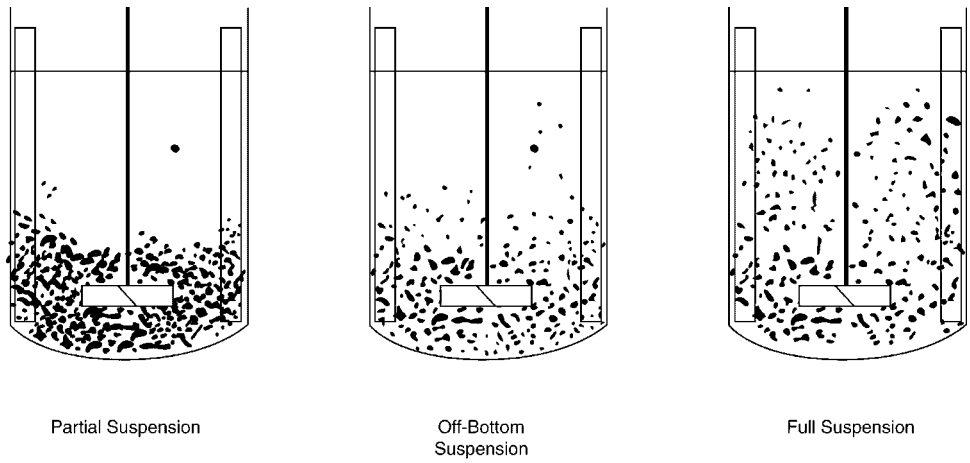

Fig. 23. Different degrees of solids suspension.

Table 8. **Values of Zwietering constant for Different Impellers**

	Rushton		PBT		HE3	
C/T	D/T=1/2	D/T=1/3	D/T=1/2	D/T=1/3	D/T=1/2	D/T=1/3
1/3	4.72	8.37	4.97	6.95	7.14	10.41
1/4	4.2	7.43	4.74	6.64	6.82	9.95

point of off-bottom suspension. With further increase in mixer power, k_L still increases but at a slower rate providing reduced incremental benefit. Impeller speed for off-bottom suspension, N_c, is the most important parameter in designing mixers.

The correlation for N_c based on experimental data has been well researched. The pioneering work was carried out by Zwietering in 1958 and a correlation with different impeller types and tank sizes was developed (6):

$$N_c = s\nu^{0.1}D_p^{0.2}D^{-0.85}\left(\frac{g\Delta\rho}{\rho}\right)^{0.45}C_s^{0.13}$$

where ν is kinametic viscosity and C_s is percent solids concentration.

The dimensionless constant s depends on impeller type and configuration and its values for three different impellers are given in Table 8. Values of "s" for several other impellers can be obtained from the literature. Other researchers have since developed similar correlations that include effects of a few additional parameters such as D/T, C/D, and H_l/T. The corresponding exponents of these parameters vary in range: -1 to -1.7 for D/T, 0.15 to 0.2 for C/D, and $\sim$0.33 for H_l/T.

Some studies (7) have been carried out to measure distribution of solids in mixing tanks. Local solids concentrations at various heights are measured at different impeller speeds. Typical data (Fig. 24) demonstrate that very high mixer speeds are needed to raise the solids to high levels. At low levels, solids concentration can exceed the average concentration within a range of mixer speeds when solids are suspended but not well distributed. These solids distributions depend on the impeller diameter, particle size, and physical properties of both phases.

Note that when solids are sticky and/or have tendency to agglomerate, predictions for their suspension may be adversely impacted. Mixing of such solids should be experimentally studied to determine requirements of shear and energy.

5.2. Floating Solids. There are several applications where solids are lighter than the carrying liquid and can also be sticky at process conditions. These solids either have density less than that of the liquid or are highly porous or are nonwetting. In order to keep these particles from rising to the surface and agglomerating, pulling down action must be provided by the mixer. Such floating solids are encountered in polymeric processes and in slurrying of difficult-to-wet porous solids.

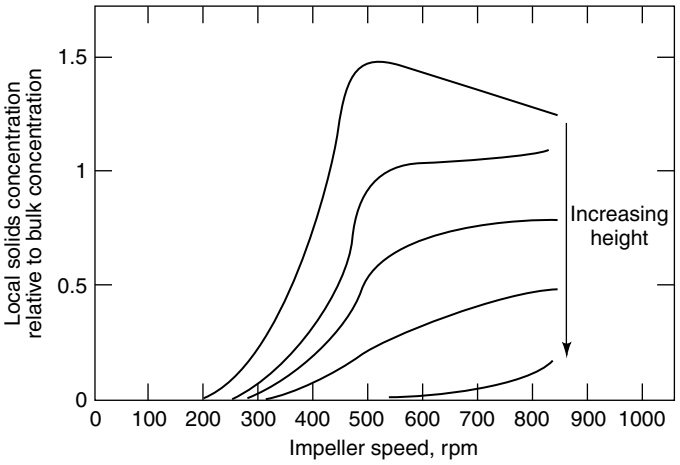

Fig. 24. Solids concentration vs impeller speed at different heights.

The mechanism for entrainment of floating solids is quite different from that for suspension of heavy solids, and requires much higher mixing energy. A force balance on a floating particle (8) about to be incorporated consists of an upward buoyant force opposed by downward drag and lift forces. For entrainment to occur, a net downward force is required. Observations of the motion of floating solids have revealed that liquid swirl created in unbaffled tanks equipped with downpumping axial flow impellers, provides these necessary forces. Tanks with full baffles (width = $T/12$) and same impellers do not have such a swirl (Fig. 25**a**). The swirl produces centrifugal forces that move the light particles along the liquid surface radially into the cone of the vortex where velocities are high enough to cause entrainment. This swirl can be created by using modified baffles such as a single wide baffle near the liquid surface (Fig. 25**b**), full length baffles having width equal to one-fiftieth of the tank diameter (Fig. 25**c**), and $T/12$ wide baffles ending below the liquid level (Fig. 25**d**).

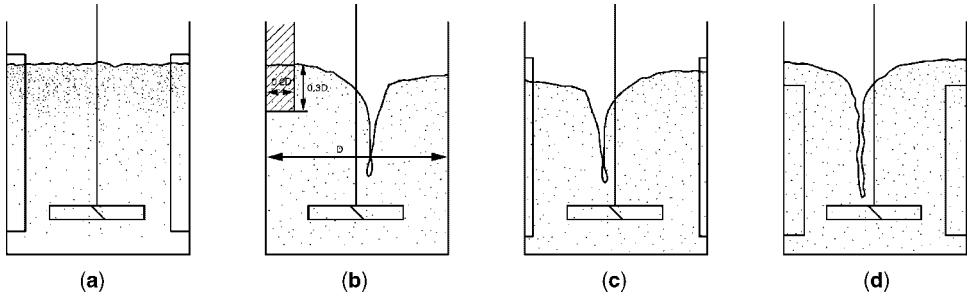

Fig. 25. Mixing of floating solids in agitated tanks with downpumping axial flow impellers: (**a**) full baffles width = $T/12$, no surface movement; (**b**) single wide baffle at liquid level, precessing vortex; (**c**) partial baffles width = $T/50$, precessing vortex; and (**d**) submerged partial baffles, narrow vortex.

There are other equally effective partial baffles that vary in configuration, eg, finger baffles of different shapes positioned at the surface. Scale-up to maintain equivalent vortex depth is based on maintaining a constant Froude (Fr) number, N^2D/g, which results in increasing the mixer tip speed in proportion to $T^{0.5}$. For the single wide baffle design (Fig. 17**b**), the constant Froude number can be determined from

$$Fr = 0.036\ (D/T)^{-3.65}(\Delta\rho/\rho_1)^{0.42}$$

While a swirl is required to entrain floating solids, excessive swirl can induce vapors from the head space that can be undesirable in some cases. These entrained vapor bubbles lower mixer power consumption and in general reduce mixing quality. A mixing system consisting of uppumping axial flow impellers in vessels with full baffles can be used to entrain floating solids. The entrainment under these flows occurs near the wall on the liquid surface. Vapor entrainment can thus be minimized since a deep swirl is not formed.

6. Immiscible Liquid–Liquid Mixing

Mixing of immiscible liquids is frequently encountered in chemical, petroleum, pharmaceutical, cosmetics, food, and mining industries. Several reacting and nonreacting systems include extraction (qv), alkylation (qv), nitration, sulfonation, halogenation, suspension polymerization, emulsifications, and phase-transfer catalysis (see CATALYSIS, PHASE-TRANSFER). When mutually insoluble liquids are mixed in an agitated tank, a dispersion of one phase is produced, thereby increasing the interfacial area manyfold. For example, in a 1320-liter (350-gal) tank an interfacial area of 4047 m^2 (1 acre) is achieved with equal volumes of the two phases and 1-mm diameter dispersed drops. Mixing energy spent in maximizing this interfacial area is generally cheaper than the resultant benefit from enhancement in the mass-transfer rate. However, optimization of mixing energy is necessary because too much energy can result in formation of undesirable emulsions, increasing temperature and reducing product quality. In order to design a mixer for a given process, it is important to define the process needs, eg, homogenization of phases, fine dispersions for fast reacting systems, dispersions with narrow drop sizes, minimize diffusional resistance in the continuous phase, induce convection within the drops, generate very fine stable emulsions, etc.

When an impeller is rotated in an agitated tank containing two immiscible liquids, two processes take place. One consists of breakup of dispersed drops due to shearing near the impeller, and the other is coalescence of drops as they move to low shear zones. The drop size distribution (DSD) is decided when the two competing processes are in balance. During the transition, the DSD curve shifts to the left with time, as shown in Figure 26. Time required to reach the equilibrium DSD depends on system properties and can sometimes be longer than the process time.

Drop breakage occurs when surrounding fluid stresses exceed the surface resistance of drops. Drops are first elongated as a result of pressure fluctuations

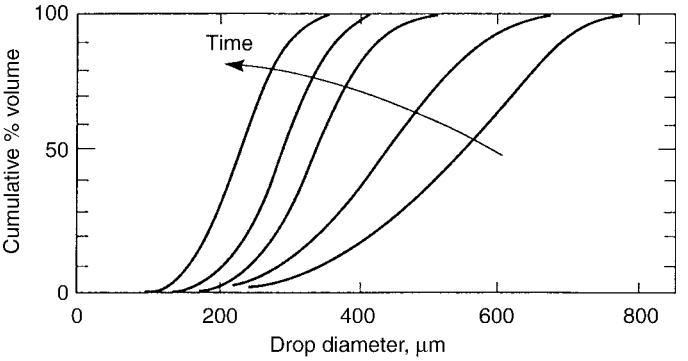

Fig. 26. Variation in drop size distribution with time.

and then split into small drops with a possibility of additional smaller fragments (Fig. 27). Two types of fluid stresses cause dispersions, viscous shear and turbulence.

1. In considering *viscous shear* effects, it is assumed that the drop size is smaller than the Kolmogoroff microscale $\eta = [v^3/\epsilon]^{1/4}$. The largest drop $d_{\max}$ that can exist in a shear field is related to the maximum value of the shear rate by

$$d_{\max} = \frac{2\sigma(p+1)f(\mathrm{p})}{\dot{\gamma}_{\max}\mu_c(1.19p+1)}$$

   where σ is interfacial tension, p is the viscosity ratio of dispersed to continuous phase (9), $\dot{\gamma}_{\max}$ is maximum shear rate and μ_c is viscosity of continuous phase. The function $f(p)$ has been experimentally determined (10).
2. Drop breakup by *turbulence* occurs when fluid turbulent energy exceeds the stabilizing surface energy of drops. The dispersed drops are larger than Kolmogoroff microscale η• Φωρ ινισψιδ δρωπσ τϑε μαξιμυμ σταβλε δρωπ διαμετερ ισ δετερμινεδ βθ εδυατινγ τϑε τχω ενεργιεσ ανδ ψαν βε εξ πρεσσεδ ασ φωλλωχσ≡

$$d_{\max} \alpha (\sigma/\rho_c)^{0.6}\varepsilon_{\max}^{-0.4}$$

   where ρ_c is density of continuous phase and $\epsilon_{\max}$ is maximum energy dissipation rate per unit mass. It has been experimentally determined that

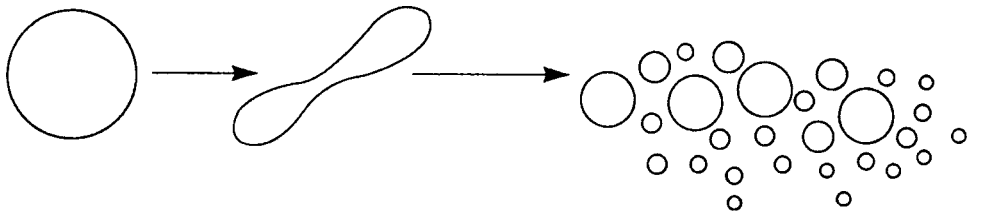

Fig. 27. Breakup of dispersed drops.

Sauter mean diameter of drops d_{32} is proportional to d_{max}, and since average ϵ is related to ϵ_{max},

$$d_{32} \alpha (\sigma/\rho_c)^{0.6} \epsilon^{-0.4}$$

Also ϵ is proportional to mixer P/V, ie, N^3D^2, and therefore

$$d_{32}/D \alpha We^{-0.6}$$

where We = Weber number = $\rho N^2 D^3/\sigma$

Drops coalescence is caused by collision of dispersed drops and drainage of liquid trapped between them. Coalescence frequency can be defined as the product of collision frequency and efficiency per collision. The collision frequency depends on number of drops and flow parameters such as shear rate and fluid forces. The collision efficiency is a function of liquid drainage rate, surface forces, and attractive forces such as van der Waal's. If contact time between drops is too short for the liquid to drain, the drops can separate.

When significant coalescence occurs along with breakup, eg, in concentrated dispersions where $0.01 < \Phi < 0.3$; turbulence is affected by phase fraction Φ. Therefore stresses responsible for drop breakup are reduced and the drop size increases. It has been demonstrated that this effect on drop size can be expressed as

$$d_{32}/D = C_3(1 + C_4\Phi)We^{-0.6}$$

C_4 is termed the turbulence damping factor because of high holdup, and its reported values vary in the 2.5–5.4 range. The proportionality constant C_3 depends on impeller type and diameter. Figure 28 shows the effect of dispersed phase fraction on the drop size for two impeller types.

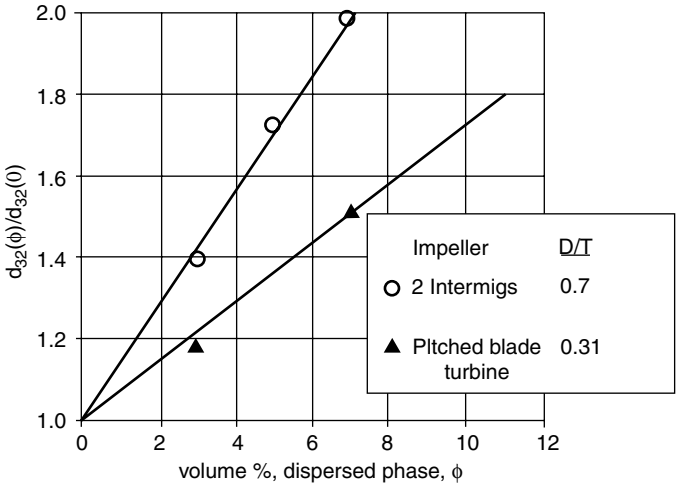

Fig. 28. Effect of dispersed phase fraction on drop size for 2 Intermig and PBT $d_{32}(0)$ represents Sauter mean diameter at low phase fraction.

If dispersed drops are viscous, the internal viscous resistance to deformation can impact the drop size. By equating turbulent stress with sum of viscous and surface stresses one can show that

$$d_{32}/D = C_1\ We^{-0.6}\ [1 + C_2\ V_i(d_{32}/D)^{1/3}]^{0.6}$$

where $V_i = (\rho_c/\rho_d)^{1/2}\mu_d ND/\sigma$ represents ratio of viscous to surface forces stabilizing the drop. Values of constants C_1 and C_2 have been experimentally measured be Calabrese and co-workers for different liquid systems and are 0.054 and 4.42, respectively.

6.1. Dispersion Measurement. Several laboratory techniques have been successfully used to measure dispersion qualities that include phase homogenization, freezing of drops, direct photography, light transmittance, reaction/mass transfer, and conductivity. Homogenization is the simplest technique and is applicable when mass-transfer rate is less important. The experiments are carried out by observing the location of the interface as mixer speed is increased in a transparent tank. This measurement is aimed at determining the minimum agitator speed for homogeneous dispersion.

Dispersed drops in a mixing tank can be frozen by forming a protective film around them, thereby preventing coalescence. A sample of stabilized emulsion can then be drawn and optically analyzed for drop size distribution. The protective film around the drops can be formed by a reaction of polyacrylic acid in the aqueous phase and polyisobutylene succinic acid in the oil phase. There are other reactions that are equally effective.

Direct photography of drops is done with the use of fiber optic probes using either direct or reflected light. Still or video pictures can be obtained for detailed analysis. The light transmittance method uses three components: a light source to provide a uniform collimated beam, a sensitive light detector, and an electronic circuit to measure the amplified output of the detector. The ratio of incident light intensity to transmitted intensity is related to interfacial area per unit volume.

6.2. Suitable Impellers. Turbine type impellers provide the desired mixing conditions for immiscible liquids. Even in high viscosity liquid emulsifications, turbines are more effective than agitators conventionally used for blending of viscous liquids. There are two types of correlations reported in the literature (11) for these impellers, one for minimum speed for homogeneous dispersion and the other for Sauter mean diameter d_{32}. The minimum agitator speed N_m for suspension can be estimated from the following:

$$N_m = C_1\ D_2^C(\mu_c/\mu_d)^{1/9}\ \sigma^{0.3}\ \Delta\rho^{0.25}$$

The value of C_2 is around $-2/3$ and C_1 depends on impeller type and location. This correlation does not impact on drop sizes and is applicable when the system is not mass-transfer limited.

The criterion of maintaining equal power per unit volume has been commonly used for duplicating dispersion qualities on the two scales of mixing. However, this criterion would be conservative if only dispersion homogeneity is desired. The scale-up criterion based on laminar shear mechanism (10) consists

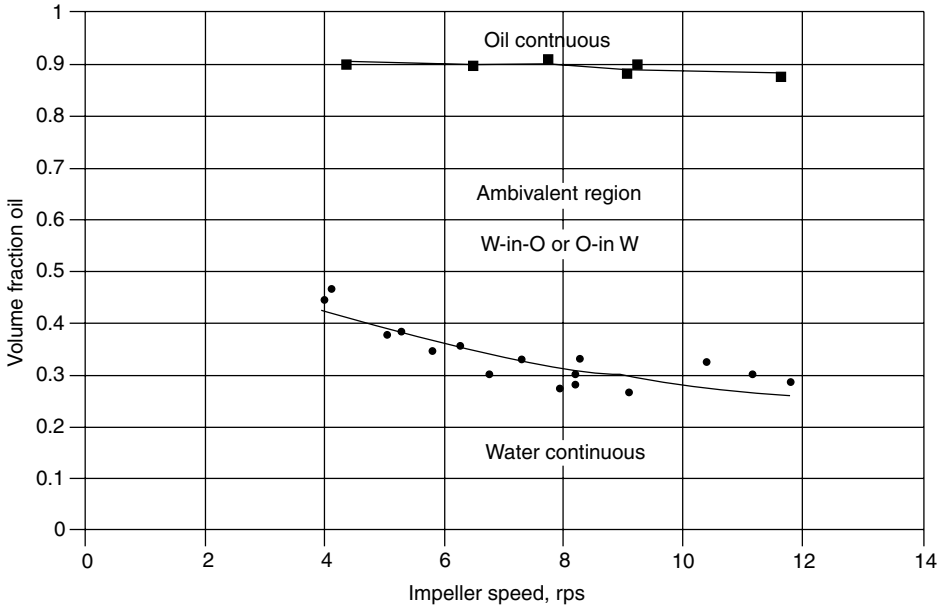

Fig. 29. Phase inversion boundaries for kerosene–water system

of constant $T^{1/2}$ $(ND)^{-3/2}$, typical for suspension polymerization. The turbulence model gives constant tip speed πND for scale-up.

6.3. Phase Inversion. This is a phenomenon caused by changing mixing conditions so that the dispersed and continuous phases interchange. The phase to become dispersed depends on the volume concentration of the two liquids, their physical properties, and the dynamic characteristics of the mixing process. There is always a range of volume fractions throughout which either component remains stably dispersed, and this is called the range of ambivalence. The limits of this range are influenced by the size and shape of the vessel, mixer speed, and physical properties of the liquids. Figure 29 shows the ambivalent region for kerosene–water system (Data of Ref. 12).

Depending on the process requirement, phase inversion may need to be avoided or may be desired. In liquid–liquid reaction processes, the reaction rate may be retarded due to phase inversions which must be prevented. When preparing very small drop size emulsions ($\sim$ 1μm), manipulating phase inversion may be necessary.

Quite often industrial liquids contain surfactants and impurities that alter interfacial tension. Such changes significantly affect the minimum agitator speed for dispersion, drop sizes and phase inversion behavior. These effects should be determined experimentally for designing mixing systems.

7. Gas–Liquid Mixing

Mechanically agitated gas–liquid contactors are widely used in industrial processes. Typical nonreacting processes include absorption and stripping, whereas

reacting systems include oxidation, hydrogenation, chlorination, etc. They are also used for carrying out biochemical processes such as aerobic fermentation (qv), manufacture of protein, and wastewater treatment. The fractional holdup of gas ϕ in these contactors is a basic measure of their efficiency. This, in conjunction with Sauter mean bubble diameter d_{32}, determines the interfacial area, $a = 6\ \phi/d_{32}$, and hence the mass-transfer rate. Knowledge of ϕ also gives the residence time for each phase. One of the most commonly used impeller is the disk flat blade turbine, also called the Rushton turbine, (Fig. 5), which can create large interfacial areas by means of the turbulent radial flow pattern. Cheminner CD6 can provide higher gas holding capaciy under certain gas sparging. Axial flow impellers and hydrofoil impellers have also been used when high liquid recirculation is desired.

Process performance of gas–liquid contactors depends on the hydrodynamic conditions inside the vessel. With radial impellers such as Rushton and CD6 impeller, various hydrodynamic conditions observed during the process of gas dispersion are flooding, loading, and complete dispersion. With axial flow impellers such as PBT, the hydrodynamic conditions include direct loading and indirect loading. These conditions depend on superficial gas velocity, impeller type and size, mixer speed, and sparger design and location.

Flooding with radial flow impellers is a flow regime dominated by buoyancy effects of gas leaving the sparger. The results of increasing mixer speed with constant gas rate have been associated with changes from flooding to loading to complete dispersion (13) (Fig. 30**a**). At flooding gas bubbles are not dispersed and recirculated by the impeller. Loading condition is in which the impeller disperses gas in the upper region of the vessel. Complete dispersion is characterized by distribution of gas bubbles throughout the vessel and significant recirculation of bubbles back into the impeller. For a low viscosity aqueous/air system while using Rushton impeller, flooding can be avoided at gas flow number $Fl = Q_g/ND^3 > 30Fr(D/T)^{3.5}$ and complete dispersion can be expected at $Fl > 13Fr^2(D/T)^5$. The parameter Q_g is the gas sparging rate and Fr is the Froude number $= N^2D/g$.

A general flow map of different hydrodynamic conditions consists of regions of flooding, loading, and complete dispersion on a plot of N versus Q_g for a Rushton turbine shown in Figure 31.

When using a downpumping PBT in low viscosity liquids, gas–liquid flow regimes of direct loading and indirect loading are above flooding condition. As shown in Fig. 30, direct loading occurs when gas bubbles rise from sparger to the impeller blades before recirculation in the bulk. Under indirect loading liquid pumped by the impeller overcomes buoyancy of the bubbles and they are swept away and recirculated. Under direct loading conditions, severe mechanical vibrations of the mixer can occur due to opposing forces. This operating difficulty can be avoided by reversing the mixer rotation to pump upward.

When an impeller is rotated in a gas-sparged liquid-filled tank, it creates rapidly spinning trailing vortices behind the impeller blades. These vortices contain centrifugal force fields and shear rates, and lead to pressures low enough to form vortex cavities. As the aeration number ($Fl = Q_g/ND^3$) is increased (Fig. 32), the vortex cavities change size and shape from clinging cavities (Fig. 32**a**) to large cavities (Fig. 32**b**), alternating 3–3 cavities (Fig. 32**c**), until they bridge

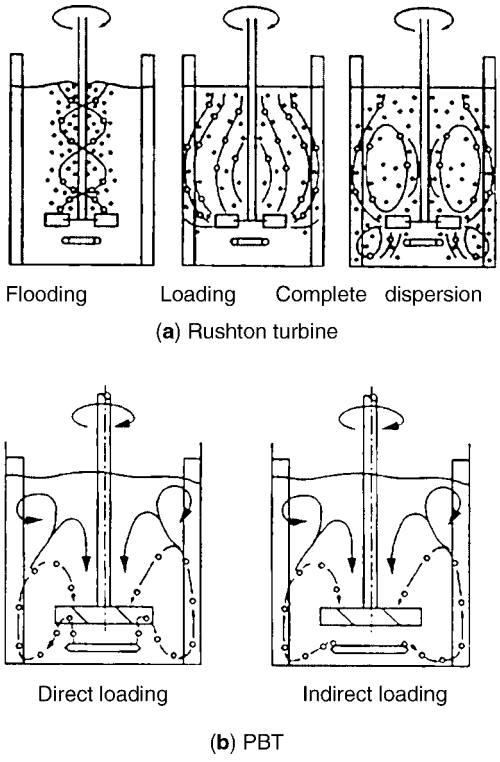

Fig. 30. Bulk flow patterns with incresing N at constant Q_g, where (**a**) shows flooding, loading, and complete dispersion with Rushton, and (**b**) shows direct loading and indirect loading with PBT

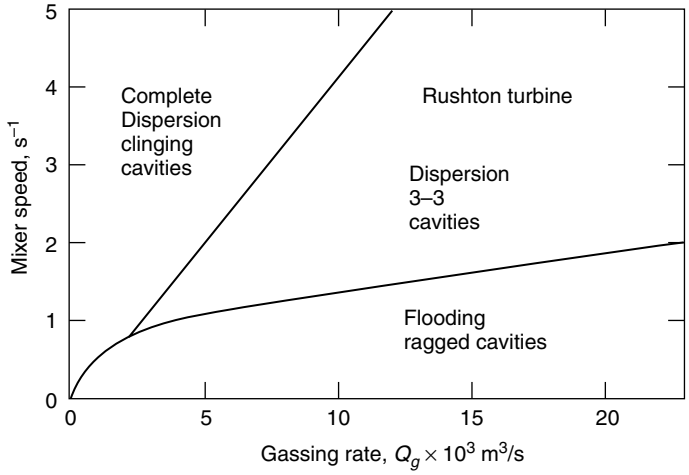

Fig. 31. General flow map of a gas-sparged agitated tank.

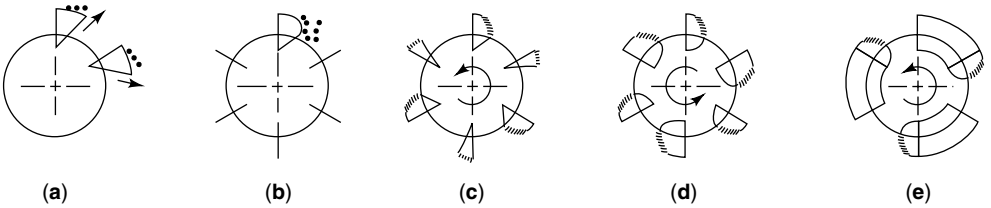

Fig. 32. Cavity formations behind impeller blades where (**a**) illustrates clinging cavities, (**b**) a large cavity, (**c**) 3–3 cavities, (**d**) alternating large and large cavities, and (**e**) bridging cavities

from one blade to the next (Fig. 32**e**). Shapes of vortex, clinging and large cavities are shown in Figure 33.

Mixer power under gassed conditions, P_g, varies as Fl is increased as shown in Figure 34. The initial small drop in power consumption is associated with limited reduction in the pumping capacity of the turbine as the gas bubbles in the vortex cavities increase in size. If gas throughput is further increased, at an $Fl = 0.025$, there is a clear point of inflection in the curve which is associated with formation of alternating large and clinging cavities. The Fl alone is not sufficient to correlate P_g because the curves shown in Figure 34 are different at different mixer speeds, higher at lower speeds (14).

With CD6 impeller, onset of cavity formation occurs at higher gas rate than with Rushton impeller. Also cavities tend to be smaller, leading to lower drop in power consumption P_g as shown in Figure 35. This means that CD6 can disperse more gas compared to Rushton impeller prior to reaching flooding conditions. This is demonstrated in the flowmap (Fig. 36) showing flooding region for CD6 at much higher flow number. Both impellers, however, provide unsatisfactory gas dispersion at $Fr < 0.045$.

Gas holdup with Rushton turbine can be estimated from the following correlation:

$$\phi = 0.1(D/T)^{1.25}(ReFrFl)^{0.35}$$

At a given gas sparging rate, interfacial area "a" is constant at low mixer speeds. When mixer speed is increased above a critical speed N, "a" starts increasing and varies linearly with N. This critical speed for Rushton turbines as determined in an O_2/sodium sulfite system, is given by the following:

$$\frac{N_o D}{(\sigma g/\rho)^{0.25}} = 1.22 + 1.25(T/D)$$

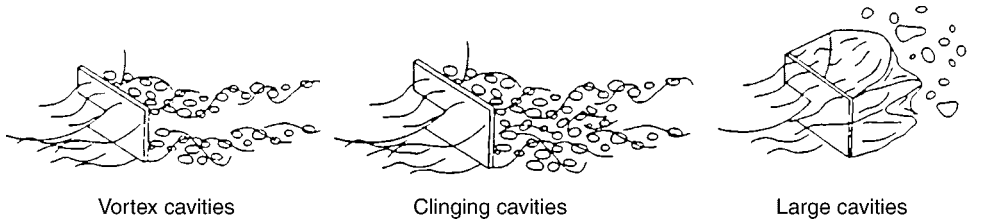

Fig. 33. Shapes of different gas cavities behind impeller blades.

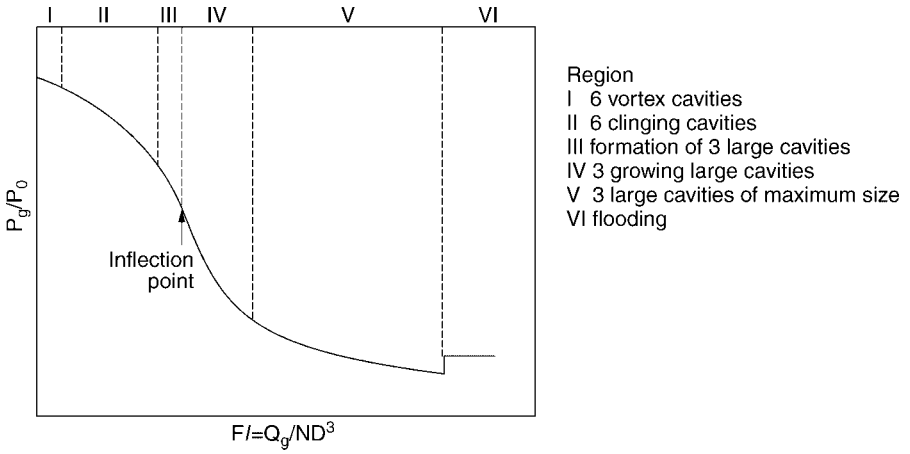

Fig. 34. Gassed power curve for constant N with increasing Q_g.

The interfacial area in the region with agitation effect $N > N_o$ and liquid height, H_l, is given by

$$\frac{aH_l}{(1-\phi)} = 0.79\mu(N - N_o)D\sqrt{\frac{\rho T}{\sigma}}$$

For optimum mixer design, ie, maximum "a" at lowest power input, small-diameter impellers at high mixer speeds should be used. Scaling up for equal "a" must be done on the basis of equal tip speed and geometric similarity. For maximizing gas holdup, it is recommended that a ring sparger of diameter equal to 0.8 D located below the impeller be used.

7.1. Gas Inducement. When the gas used in the process is hazardous and/or expensive, it is recycled from the vapor space using gas-inducing impellers. Typical applications include hydrogenation, chlorination, and phosgenation

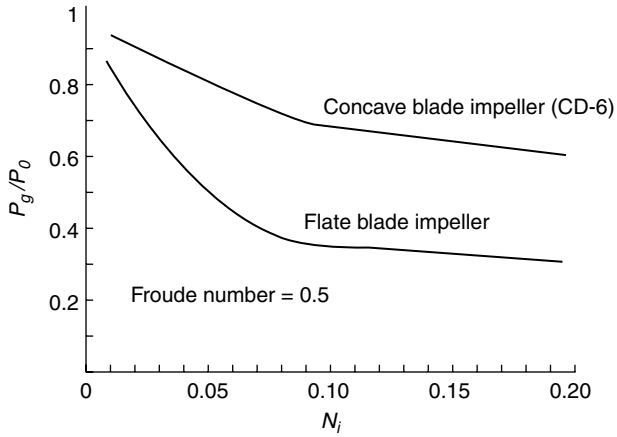

Fig. 35. The P_g/P_o curves for Rushton and CD6.

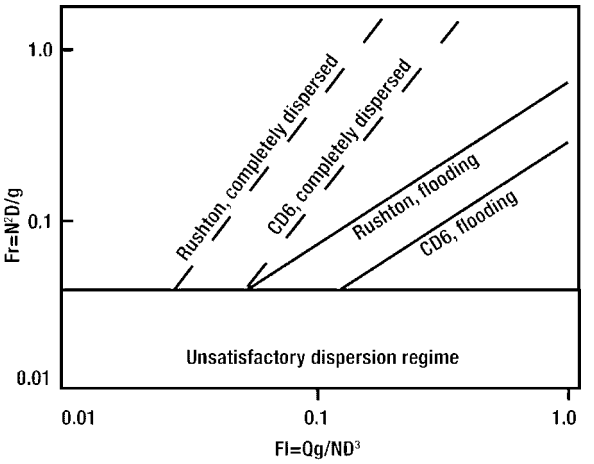

Fig. 36. Flow regime map for Rushton and CD6.

processes. There are two types of self-inducing mixing systems, hollow shaft/impeller and Praxair AGR, as shown in Figure 37. A hollow/shaft mixer uses the acceleration of the liquid phase over the blades to locally reduce the pressure at an orifice and induce a flow of gas through a hollow shaft. The critical speed at which gas flow is first induced is given by the following:

$$N_g = \sqrt{\frac{2gh_s}{k_h(\pi D)^2}}$$

where h_s is submergence of the orifice and k_h is head loss constant for different impeller types having values in the range of 0.9–1.3 (15). At speeds $> N_g$, the flow rate of induced gas Q_i increases with increasing mixer speed. Also, Q_i is higher with larger impellers. Turbine impellers require lower N_g and induce more gas compared to hydrofoil impellers.

The AGR system uses a combination of high speed helical screw impeller and draft tube to entrain vapors with a flat blade impeller rotating just below the draft tube. Scale-up of self-inducing mixers is normally on the basis of maintaining constant Froude number. This requires designing large units for very high power inputs, and therefore commercial applications of self-inducing mixers are limited.

8. Blending in Large Tanks

Blending of miscible liquids in 6–90-m (20–300-ft) diameter tanks is carried out with jet mixers and side-entering propellers (SEP). Jet mixers are used in conjunction with a pump that serves as the source of the required mixing energy. With suitable pumps, jet mixers are attractive for use in liquefied natural gas (LNG), liquefied petroleum gas (LPG), gasoline, jet fuel, and distillate fuel

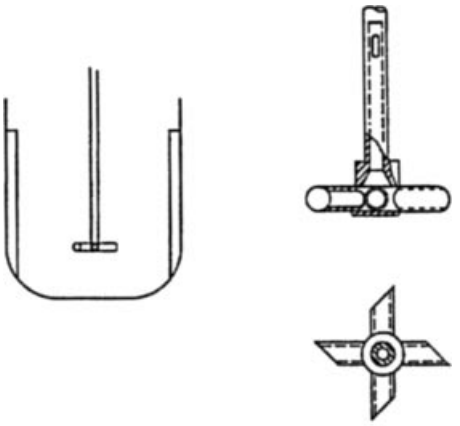

Hollow shaft/tubular blade impeller

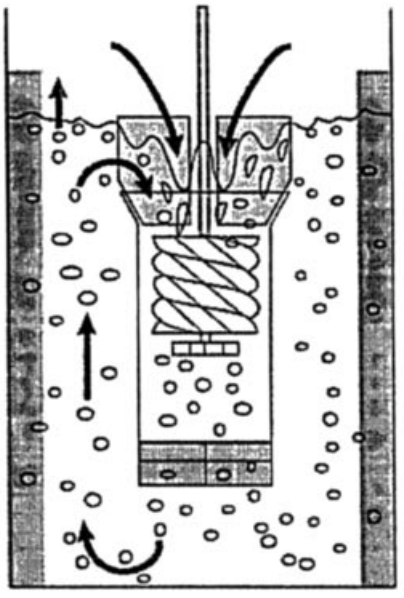

Praxair AGR

Fig. 37. Self-inducing mixing systems.

storage and blending tanks; otherwise SEP mixers must be used. The basic requirements for blending in large storage tanks are that the entire contents of the tank be mixed and that the mixing be completed in the desired time. In LNG and LPG tanks it is possible to add a dense layer to the bottom of a tank which, upon warm-up during storage, can become less dense than the upper layer. This can result in rollover of the tank contents and dangerously high vapor release rates due to spontaneous flashing. Therefore, such tanks should be adequately mixed to eliminate stratification.

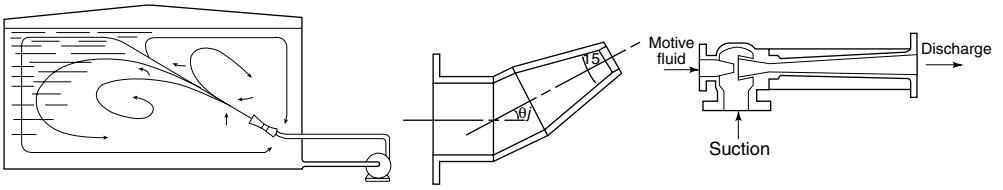

(**a**) Jet nozzle in a tank (**b**) Simple jet nozzle and eductor

Fig. 38. Types of jet nozzles and their positioning in the tank.

8.1. Jet Mixers. These mixers can be used for continuously blending miscible fluids as they enter a tank, or batchwise by recirculating a portion of the tank contents through the jet. The jet mixer is a streamlined nozzle installed in the side or center of a tank near the bottom or top. It can be pointed horizontally or at an angle diametrically across the tank (Fig. 38**a**), The nozzle design can be either a simple pipe with reduced diameter (Fig. 38**b**) or a jet eductors (Fig. 38**b**). Jet eductors provide higher entrainment of the surrounding liquid compared to simple nozzles.

Jets mix by entrainment of the surrounding fluid into the jet. The induced flow within the tank is therefore greater than the jet flow itself and can lead to rapid mixing. The amount of fluid entrained by a jet with nozzle diameter d is a function of jet $Re_j = dU_o\ \rho/\mu$, jet expansion angle, and jet length. For most effective mixing, commercial jet mixers (16,17) are designed for turbulent jet operation at $Re_j > 3000$. The minimum required nozzle discharge velocity, U_o, for heavy into light liquid is given by

$$U_o = \left(\frac{2gFH_s\Delta\rho}{\sin^2(\theta_j + 5)\rho} \right)^{1/2}$$

where H_s is submergence height of nozzle, $\Delta\rho$ is density difference between feed liquid and tank liquid, ρ is density of tank liquid, θ_j is jet inclination angle, and factor F depends on the initial condition of tank homogeneity and is calculated by the following:

For initially homogeneous tank

$$F = 0.25(\Delta\rho/\rho)^{-0.34}(H_s/d)^{0.65} \quad \text{for} \quad H_s/d \leq 100$$
$$F = 7.5(\Delta\rho/\rho)^{-0.24} \qquad \text{for } H_s/d > 100$$

For initially stratified tank

$$F = 0.59\ (H_s/d) - 4\ln(\Delta\rho/\rho) - 32.7 \quad \text{for} \quad H_s/d > 50$$

For a known flow rate the nozzle diameter is set by the largest size that satisfies the turbulent jet requirement for both heavy and light jets, ie,

$$\frac{dU_o\rho}{\mu} \geq 3000$$

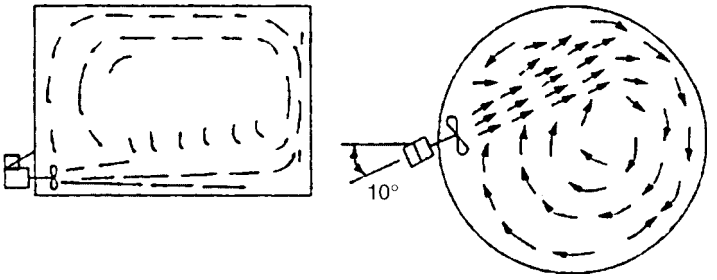

Fig. 39. Flow patterns with side-entry mixers.

Additionally, for adequate penetration of the jet across the tank, the nozzle diameter should be at least as large as that given by

$$d \geq \frac{H_s}{400 \sin \theta_j}$$

The pressure drop through a jet mixing nozzle is given by $\Delta P = 0.9\ \rho\ Q^2/d^4$. The time to achieve 95% homogeneity can be estimated from

$$U_o t_m/d = 3(Z/d)^2$$

where t_m is mixing time and Z is free jet path length until the jet hits the opposite tank wall at the liquid surface.

8.2. Side Entering Propeller Mixers (Fig. 39). Side entering propeller (SEP) mixers induce a spiral jet flow across the floor of the tank continually entraining liquid from other areas of the tank. This jet stream initially only agitates the denser liquid at the bottom, but gradually penetrates the upper layers of the tank with sufficient velocity to generate both full top-to-bottom flow and break the interface between various density strata to achieve a full homogeneous mix. This gradual breakdown of the interfaces is illustrated in Figure 40 by flow patterns and changes in liquid specific gravity as a function of blending time at different tank heights. The design of the mixer can be based on the discharge capacity of the propeller and liquid entrainment in relation to tank volume and desired blending time. For liquids having viscosity <100 mPa s, a minimum of 0.25-HP/kbbl power is required to set the whole tank in circulation. This is a necessary condition for expecting desired liquid homogeneity. Blend time can then be calculated using pumping rate of the propeller, rate of entrainment, and 3–10 turnovers depending on liquid viscosity.

The SEP mixers are also extensively used for agitation of paper stock in the pulp and paper industry, and for suspension of sludge in crude oil storage tanks in the petroleum industry.

9. Crude Tank Sludge Control

Depending on the type and concentration of sludge in petroleum crude receipt, settling of sludge can occur in crude storage tanks at a rate of 25–150-mm

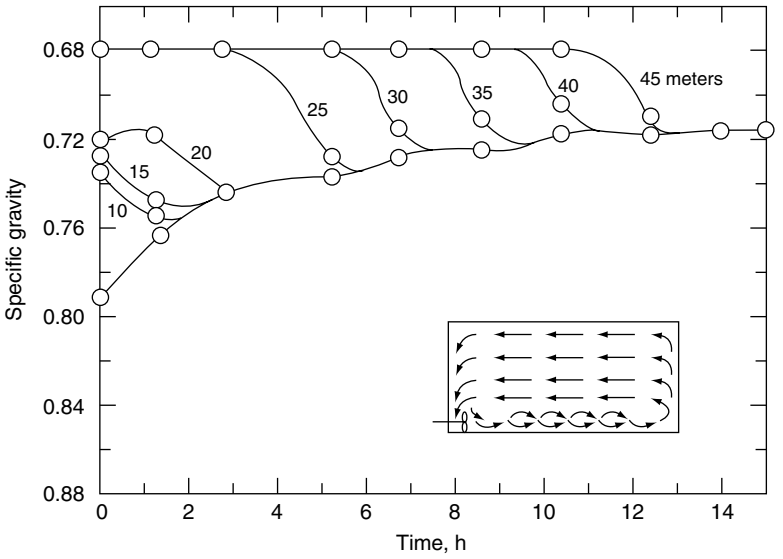

Fig. 40. Gradual breakdown of interface in a stratified tank.

height/month. Without its suspension, this sludge can harden due to packing of top layers, and/or can form mounds because of sludge shifting during crude receipts and pumpouts. Mixing energy, therefore, must be supplied on a continuous or frequent basis to maintain tank cleanliness. For achieving good on-stream sludge control, two competing technologies are available: SEP mixers and rotating jet mixers called Butterworth P-43 machines. Adequately designed and operated SEP mixers can prevent sludge settling by establishing movement of crude throughout the tank. They cannot, however, be expected to resuspend sludge accumulated for an extended period. The P-43 submerged jet nozzle system can prevent sludge accumulation and resuspend large sludge volumes. Selection of the mixing system depends on the nature of existing facilities.

SEP mixers are horizontally installed on the side of the tank and near the bottom. By rotating the propeller, a spiralling jet is produced (Fig. 39) near the tank floor that provides the desired thrust to dislodge and entrain the sediments. The SEP mixers should be designed to provide the suspension velocity at the farthest distance on the tank floor. For effective utilization of mixing energy the SEP shaft must be off-center so that the angle between the shaft and the diameter is 7–12°. With clockwise mixer rotation (looking from motor to propeller), this angle shift should be counterclockwise, resulting in tank circulation without a swirling vortex. The swirling action of liquid consumes less energy but causes sludge to concentrate at the center of the tank. In addition, tank operation is impaired at low liquid levels.

Commercial SEP mixer sizes are limited to 56 kW, and therefore more than one mixer is needed for large tanks in order to provide the desired mixing energy. The arrangement of these mixers determines the nature of the liquid circulation path. For example, clustered mixers provide a combined jet which spreads in different directions toward the opposite wall (Fig. 41). In the distributed

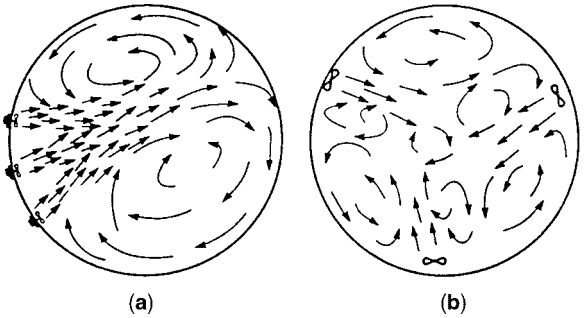

Fig. 41. Flow patterns with (**a**) clustered and (**b**) distributed mixers.

configuration, each mixer creates nearly independent liquid circulation in an arc. With both arrangements, it is recommended that mixers of the same size be used, and the number of mixers should be chosen based on the tank diameter using the following guidelines:

tank diameter, *m*	<30	30–45	45–60	>60
number of mixers	1	2	3	4 or 5

When using the clustered layout of multiple mixers, a mixer spacing of 22.5° is commonly used. It is important to position the clustered mixers opposite the crude outlet in order to benefit from liquid velocities during pump out.

With fixed-angle mixers, the sludge may be shifted to low velocity areas particularly when mixers are underpowered as shown in Figure 42. The mixer performance can then be improved by using swivel-angle mixers and operating them sequentially at different angles moving from left to right. For the same mixing quality, the power required by swivel-angle mixers is less than that required by fixed-angle mixers. For common crudes the mixer power requirement is 1.88 W/m^3. Higher mixing energy is required for heavier and waxy crudes.

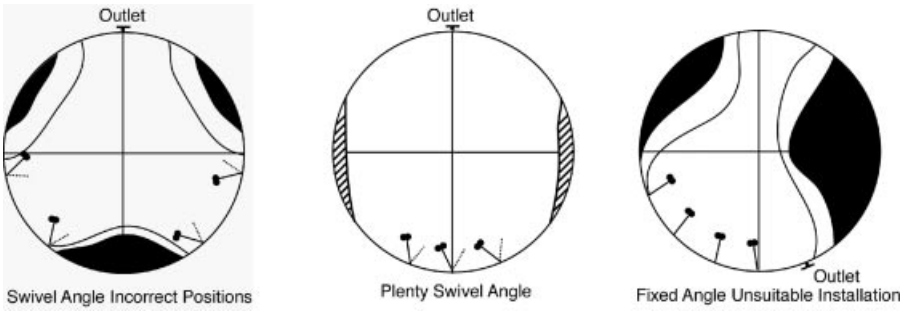

Fig. 42. Sludge shifting with improper SEP design and location.

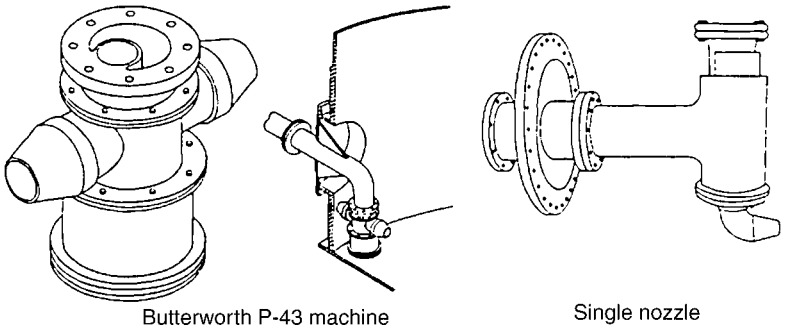

Fig. 43. Rotating submerged jet mixers.

Rotating jet mixers Butterworth P-43 system uses the rotating submerged jet concept to remove deposited sludge from crude oil storage tanks. The P-43 machine, shown in Figure 43, is a twin-nozzle jet device that directs single or opposed jets horizontally across the tank bottom. The nozzles slowly rotate to provide 360° coverage of the tank floor. The jets are designed to provide a concentrated force on the tank floor needed for suspension of settled sludge. Once suspended, the sludge is homogeneously mixed with oil and processed downstream, thus recovering its hydrocarbon value. The P-43 operation consists of pumping crude oil through the jet nozzles to provide the minimum suspension velocity at the farthest point. A portion of crude flow is directed to an impeller, which through a series of gears rotates the machine. Slow rotation of the jets, 1.5–3.5°/min, provides the necessary residence time for jet penetration through the sludge. The jets are designed on the basis of required cleaning radius R, specific gravity S, and nozzle diameter using the following correlations

$$Q = 7.56d\ R \quad \Delta P = S\{Q/26.8\ d^2\}^2$$

where d is in inches, R in feet, flow rate Q in gpm, and pressure drop ΔP in psi.

The P-43 installations can be center-mounted (CM) or shell-mounted (SM). The CM configuration uses a single P-43, but there can be different numbers of machines with a SM configuration. A CM machine is placed at the tank center and each jet is designed to suspend sludge at the tank wall with the jet cleaning radius equal to the tank radius. SM machines can be installed near the tank wall and can be single or multiple depending on tank size. A single SM machine has a cleaning radius R equal to the tank diameter T, two machines are designed for $R=T/2^{0.5}$ and three machines for $R=T/2$. Multiple SM machines can be operated sequentially with one jet at a time. The P-43 machines should be located as close to the tank floor as possible for maximum effectiveness. Tank internals such as heating coils, water drawoff lines, and roof drains should be secured to prevent dislodgement from supports by direct jet impingement.

10. Inline Motionless Mixers

When process result can be achieved in <1 min at high energy levels, use of inline motionless mixers can be significantly cost effective over agitated vessels.

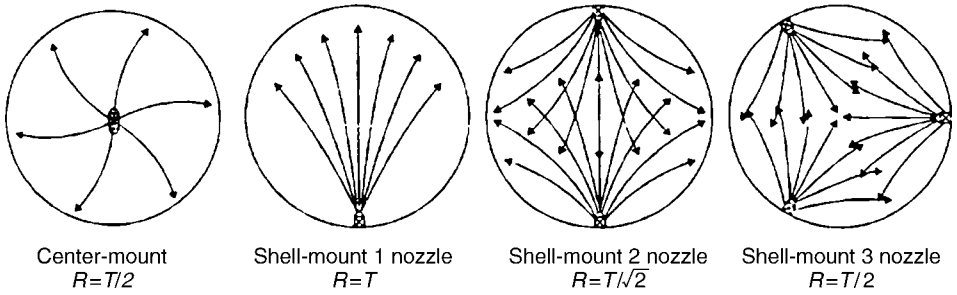

Fig. 44. Types of P-43 machine installations.

These mixers derive the fluid motion or energy dissipation needed for mixing from the flowing fluid itself. The mixing energy is simply the product of flow rate and pressure drop across the mixer. The types of in-line mixers include orifice mixing columns, mixing valves, tee mixers, and static mixers. These mixers are commonly used in chemical, petroleum, cosmetics, food, polymers, pulp and paper, wastewater industries.

Orifice mixing columns consist of a series of orifice plates contained in a pipe. The pipe normally is fabricated of two vertical legs connected by a U-bend at the bottom with orifice plates installed between flanges in the legs. Typical use is for cocurrent contacting in caustic and water-washing operations. It is generally designed at mixing energy of 5–200 kJ/m^3 (12–48 $kcal/m^3$) and contact times in the range of 10–50 s. Typical pressure drop per orifice is in the range of 5–15 kPa (37.5–112.5 mmHg).

A mixing valve in the form of a conventional globe valve is simple and economical, and can be adjusted based on changing flow rate to maintain adequate mixing energy. A typical service involves caustic washing of gas oil and water–oil mixing upstream of a desalter. The valve is normally specified to handle a pressure drop in the range of 20–350 kPa (0.2–3.5 atm).

Static mixers are used in the chemical industries for plastics and synthetic fibers, eg, continuous polymerization, homogenization of melts, and blending of additives in extruders; food manufacture, eg, oils, juices, beverages, milk, sauces, emulsifications, and heat transfer; cosmetics, eg, shampoos, liquid soaps, cleaning liquids, and creams; petrochemicals, eg, fuels and greases; environmental control, eg, effluent aeration, flue gas/air mixing, and pH control; paints for blending variety of dispersions; chemical processes for achieving pipeline uniformity before sampling.

These motionless mixers provide complete transverse uniformity and minimize longitudinal mixing, therefore their performance approaches perfect plug flow conditions. They consist of repeated structures called mixing elements attached inside a pipe. These mixing elements alternately divide and recombine fluids passing through. As a result they create shearing action at the cost of pressure drop which causes mixing of single- and multiphase systems.

Static mixers are usually classified as operating either in laminar or turbulent flow regimes. There are many proprietary designs marketed, a few are shown in Figure 45. These mixers generate a process of division, rotation, and reversal of fluid which create shear and mixing. For *blending of miscible liquids*, homogeneity is accomplished by producing striations (Fig. 46). The number of

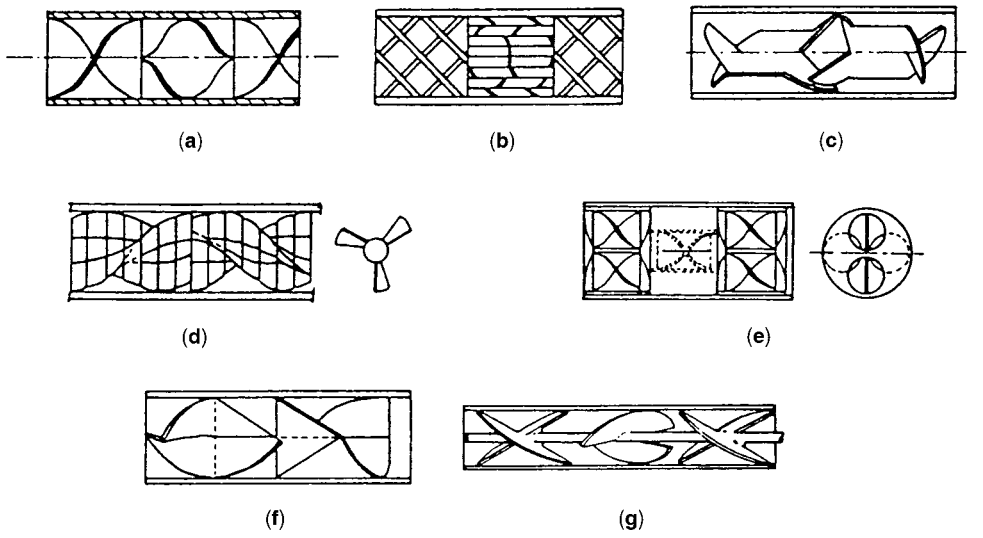

Fig. 45. Various proprietary static mixer designs: (**a**) Kenics, (**b**) Sulzer SMX (**c**) Komax, (**d**) Lightnin, (**e**) Toray Hi-Mixer, (**f**) Etoflo, and (**g**) Ross LLPD.

striations is equal to 2^n, where n is number of elements. There are other designs that produce a greater number of striations.

The energy P consumed by a static mixer is given by $P = Q\Delta P_{\mathrm{sm}}$, where Q is flow rate and ΔP_{sm} is pressure drop across the mixer. This energy is supplied by the pump used to create flow of the fluid through the mixer. For homogenization of two or more liquids, static mixers reduce standard deviation or variance. The reduction of variance is a product of shear rate and time, and therefore equal to L/D_s, where L and D_s are length and diameter of static mixer, respectively. The pressure drop depends on flow rate and liquid viscosity. For a Kenics mixer, ΔP_{sm} is about six times that of an empty pipe in laminar flow; for a Sulzer SMX mixer it is 64 times higher.

The degree of mixing is described as coefficient of variation $CoV = \sigma_s/\overline{X}$ where σ_s is standard deviation, X is fraction of additive, and $\overline{X}$ is average fraction of additive.

$$\sigma_s \text{ of unmixed liquid} = [X(1-X)]^{0.5}$$

$$\text{initial } \sigma_s/\overline{X} = [(1-X)/X]^{0.5}$$

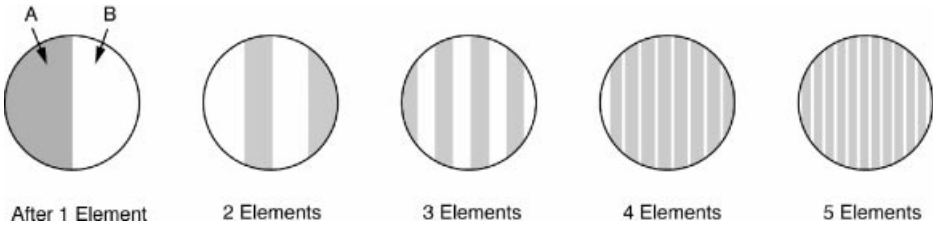

Fig. 46. Mechanism for laminar blending in Kenics static mixer (**a**) after one element, (**b**) two elements, (**c**) three elements, (**d**) four elements, and (**e**) five elements.

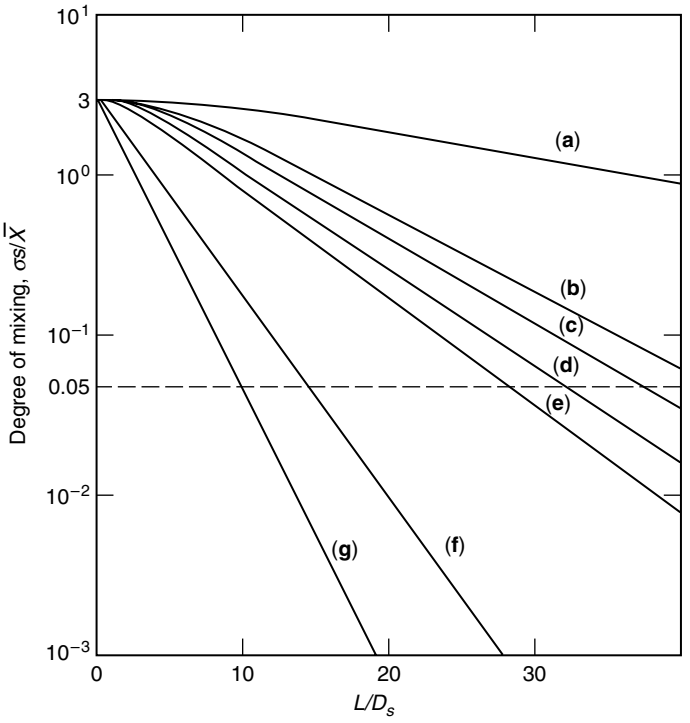

Fig. 47. Comparison of mixing rates with different static mixers in laminar flow: (**a**) Lightnin; (**b**) Komax; (**c**) Etoflo HV; (**d**) Kenics; (**e**) SMXL; (**f**) Hi-mixer; and (**g**) SMX. Satisfactory homogeneity occurs at $\sigma_s\,\overline{X}=0.05$.

If the material starts with an additive composition of 10% ($X = 0.1$) corresponding to an initial variation coefficient of 3, the variance is reduced logarithmically as L/D_s increases. Figure 47 shows a comparison of the degree of mixing produced by various static mixers as a function of L/D_s in laminar flow. These mixers appear to give markedly different performance, but when compared on a ΔP_{sm} basis are almost equivalent. Many manufacturers suggest that satisfactory homogeneity is when $\sigma_s/\overline{X}$ is reduced to 0.05. In many applications lower $\sigma_s/\overline{X}$ may be required. The exact degree of mixing depends on the product and must be determined by experience and experimentation. The smaller the amount added the larger the initial variation coefficient and the more reduction required to achieve a certain degree of uniformity. When the ratio of viscosity of additive to the main liquid is > 10, mixing becomes much harder as the additive slips past the main stream. Mixers with high ΔP_{sm} handle this better than those with low ΔP_{sm}.

Pressure drop in static mixers depends very strongly on geometric arrangement of the inserts. It is simply defined in relation to the pressure drop ΔP in an empty tube given by Darcy's equation:

$$\Delta P = \frac{5f\rho L v^2}{g_c D_s} \qquad \Delta P_{\mathrm{sm}} = K\Delta P$$

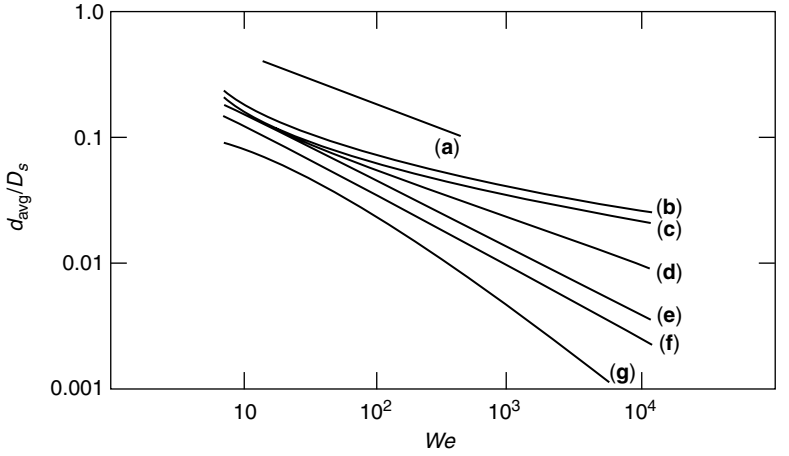

Fig. 48. Dimensionless drop size versus Weber number: (**a**) empty pipe at μ_d/μ_c=1; (**b**) through **g**, Kenics mixer at $\mu_d/\mu_c = 25$, 10, 2, 1, 0.75, and 0.5, respectively.

K depends on the mixer type and its value can be obtained from the vendor literature.

Static mixing of immiscible liquids can provide excellent enhancement of the interphase area for increasing mass-transfer rate. The drop size distribution is relatively narrow compared to agitated tanks. Three forces are known to influence the formation of drops in a static mixer: shear stress, surface tension, and viscous stress in the dispersed phase. Dimensional analysis shows that the drop size of the dispersed phase is controlled by the Weber number. The average drop size, d_{avg}, in a Kenics mixer is a function of Weber number $We = \rho_c v^2 d_h/\sigma$, and the ratio of dispersed to continuous-phase viscosities (Fig. 48), where ρ_c is density of continuous phase, v is liquid velocity, d_h is hydraulic diameter of static mixer, and σ is interfacial tension. The hydraulic diameter is defined as cross sectional area divided by wetted perimeter.

Under turbulent flow conditions, the Sauter mean diameter from two static mixers can be obtained from the following:

$$\text{Koch/Sulzer SMV} \qquad d_{32}/d_h = 0.21We^{-0.5}Re^{0.15}$$

$$\text{Kenics} \qquad d_{32}/d_h = CWe^{-0.6}Re^{0.1} \text{ for } Re > 3000$$

where Re is Reynolds number $Re = \rho_c v d_h/\mu_c$, and C is a constant that depends on mixer type.

Static mixing of gas–liquid systems can provide good interphase contacting for mass transfer and heat transfer. Specific interfacial area for the SMV (Sulzer) mixer is related to gas velocity v_g and gas holdup ϕ by the following:

$$a = C_5 v_g^{0.85} \phi^{0.15}$$

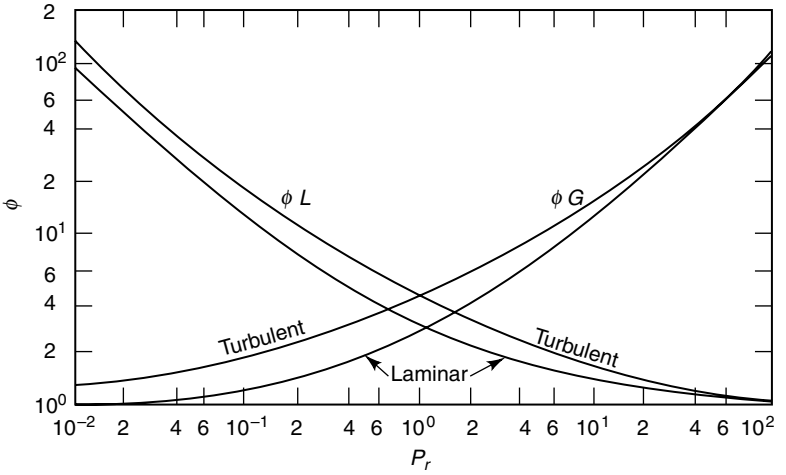

Fig. 49. The functions ϕ_L and ϕ_G plotted against the pressure drop ratio P_r.

The constant C_5 depends on the hydraulic diameter of the static mixer. The mass-transfer coefficient expressed as a Sherwood number $Sh = k_L d_h/D$ is related to the pipe Reynolds number $Re = D_s \upsilon \rho/\mu$ and Schmidt number $Sc = \mu/\rho D_s$ by $Sh = 0.0062 Re^{1.22} Sc^{1/3}$.

The pressure drop for gas–liquid flow is determined by the Lockhart–Martinelli method. It is assumed that the ΔP for two-phase flow is proportional to that of the single phase times a function of the single-phase pressure drop ratio P_r.

$$\Delta P_{sm} = \phi_L^2 \Delta P_L = \phi_G^2 \Delta P_G$$

The functions ϕ_L and ϕ_G are plotted against the pressure drop ratio P_r in Figure 49.

Heat transfer in static mixers is intensified by turbulence created by inserts. For the Kenics mixer, the heat-transfer coefficient h is two to three times greater than in an empty pipe, whereas for Sulzer mixers it is five times greater, and for polymer applications it is 15 times greater than the coefficient for low viscosity flow in an open pipe.

11. Heat Transfer in Agitated Tanks

Frequently, the contents of an agitated vessel must be heated or cooled to a given operating temperature by heat transfer to or from the fluid in the vessel. Agitators that force large amounts of fluid to circulate near the heat-transfer surfaces provide the most efficient heat transfer. In the case of close-clearance impellers used for high viscosity liquids, heat transfer is promoted by thinning of the stagnant fluid layer near the wall. Rubber scrapers can be attached to these impellers to keep the wall surface free from deposits.

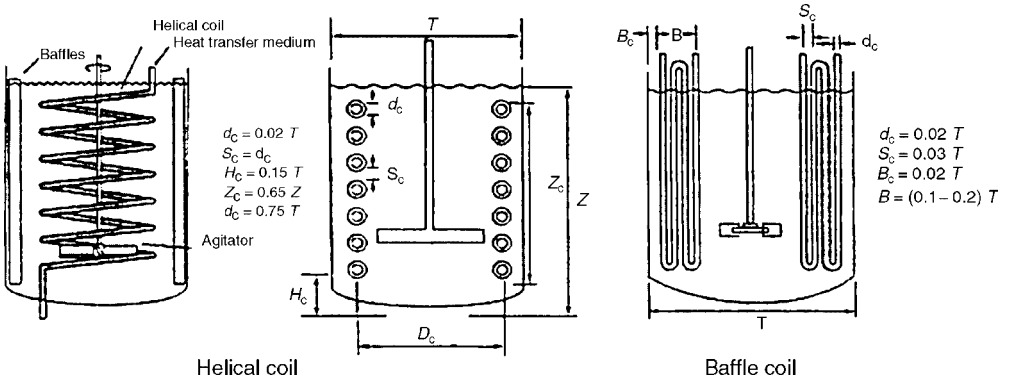

Fig. 50. Internal coil configurations for heat-transfer surfaces: (**a**) helical coil where $D_c = 0.02\text{T}$, $S_c \geq d_c$, $H_c = 0.15$ T, and $Z_c = 0.65Z$; (**b**) baffle coil where $d_c = 0.02T$, $S_c = 0.03T$, $B_c = 0.02T$, and $B = 0.2T$.

Commonly used heat-transfer surfaces are *internal coils* and *external jackets*. Coils are particularly suitable for low viscosity liquids in combination with turbine impellers, but are unsuitable with process liquids that foul. Internal coils can be either helical or baffle coils (Fig. 50). Jackets are effective for both turbine impellers for low and medium viscosity fluids, and when using close-clearance impellers for high viscosity fluids. For jacketed vessels, wall baffles should be used with turbines if the fluid viscosity is <5 Pa s (5000 cP). For vessels equipped with coils, wall baffles should be used if the clear space between turns is at least twice the outside diameter of the coil tubing and the fluid viscosity is <1 Pa s (1000 cP). Otherwise the baffles should be located inside the coil helix. A conventional jacket consists of a vessel outside the main vessel with a gap for the flow of heat-transfer fluid. Jackets can be either on the cylindrical portion of the vessel and/or outside of the bottom head. Half-pipe jackets are useful for high pressures up to 4 MPa (600 psi). They are better for liquid than for vapor service fluids and can be easily zoned. Dimple jackets are suitable for larger vessels and process conditions up to 2 MPa (300 psi) and 370°C.

The rate of heat-transfer q through the jacket or coil heat-transfer area A is estimated from log mean temperature difference ΔT_m by $q = U\,A\,\Delta T_m$. The overall heat-transfer coefficient U depends on thermal conductivity of metal, fouling factors, and heat-transfer coefficients on service and process sides. The process side heat-transfer coefficient depends on the mixing system design (18) and can be calculated from the correlations for turbines as follows:

External jackets

$$h_j \frac{T}{k} = Nu = 1.4\ Re^{2/3} Pr^{1/3} \left(\frac{\mu}{\mu_\omega}\right)^{0.14} \left(\frac{D}{T}\right)^{-0.3} \left(\frac{W}{T}\right)^{0.45} n^{0.2} \left(\frac{C}{Z}\right)^{0.2} \left(\frac{H_l}{T}\right)^{-0.6} (\sin\,\alpha)^{0.5}$$

Inernal coils

$$h_c \frac{T}{k} = Nu = 2.68\ Re^{0.56} Pr^{1/3} \left(\frac{\mu}{\mu_\omega}\right)^{0.14} \left(\frac{D}{T}\right)^{-0.3} \left(\frac{W}{T}\right)^{0.3} n^{0.2} \left(\frac{C}{Z}\right)^{0.15} \left(\frac{H_l}{T}\right)^{-0.5} (\sin\,\alpha)^{0.5}$$

Baffle coils

$$h_c \frac{d_c}{k} = Nu = 0.1\ Re^{0.65} Pr^{1/3} \left(\frac{\mu}{\mu_\omega}\right)^{0.14} \left(\frac{D}{T}\right)^{1/3} n^{-0.2}$$

Anchors

$$h_j \frac{T}{k} = Nu = 1.5\ Re^{0.5} Pr^{1/3} \left(\frac{\mu}{\mu_\omega}\right)^{0.14} \quad \text{for } Re < 200$$

$$h_j \frac{T}{k} = Nu = 0.36\ Re^{2/3} Pr^{1/3} \left(\frac{\mu}{\mu_\omega}\right)^{0.14} \quad \text{for } Re > 200$$

Effect of anchor pitch p

$$h_j \frac{T}{k} = A Re^{a} Pr^{1/3} \left(\frac{\mu}{\mu_\omega}\right)^{0.14}$$

$$a = 0.33 \quad \text{for } 1 < Re < 10$$

$$= 0.5 \quad \text{for } 10 < Re < 100$$

p/D	0.33	0.5	1.0
A	1.56	1.25	0.66

Helical ribbons

$$h_j \frac{T}{k} = Nu = 4.2\ Re^{1/3} Pr^{1/3} \left(\frac{\mu}{\mu_\omega}\right)^{0.2} \quad \text{for } 100 < Re < 1000$$

$$h_j \frac{T}{k} = Nu = 0.42\ Re^{2/3} Pr^{1/3} \left(\frac{\mu}{\mu_\omega}\right)^{0.14} \quad \text{for} < Re < 1000$$

where h_j and h_c are process side heat-transfer coefficients with jacket and coils, respectively, T is tank diameter, k is thermal conductivity of fluid, Nu is Nusselt number, Re is Reynolds number, Pr is Prandtl number, μ and μ_w are fluid viscosity in the bulk and vessel wall, respectively, D is impeller diameter, W is impeller blade width, n is number of impeller blades, C is impeller elevation from the vessel bottom, H_1 is liquid height and α is angle of impeller blades.

For multiple turbines (i in number) the sum of impeller blade widths $\sum W_i$ should be used for W, and the average impeller height $\sum C_i/i$ should be used for C in the equations that include these terms. With turbines having different diameters on the same shaft, a weighted average diameter based on the exponents of D in the appropriate equations should be used.

When concentric banks of helical coils are used, the process side heat-transfer coefficient h for the coil bank closest to the impeller is as given by the foregoing equation. For the second and third banks, the heat-transfer coefficient is 70 and 40% of the calculated value, respectively.

For close-clearance impellers the above correlations apply to installations without scrapers. If scrapers are used, the values given by the equations should be multiplied by a factor of 1.3.

For non-Newtonian fluids the above correlations can be used with generally acceptable accuracy when the process fluid viscosity is replaced by the apparent viscosity.

For low to medium viscosity fluids (<10,000 mPa s), turbine impellers can be used to provide high velocities over the heat-transfer surfaces. Jackets should be considered first because they are external and do not interfere with mixing flow patterns. If additional heat transfer is needed, baffle coils and internal helical coils should be considered in that order. While baffle coils have lower heat-transfer area, the heat-transfer coefficient is higher than helical coils. For high viscosity fluids when using close-clearance impellers, jackets are the only heat-transfer surface feasible for use. For maximizing heat transfer for energy consumed, a helical ribbon impeller having $D/T=0.95$ and $p/D=0.25$ should be used.

12. Mixing of Dry Solids and Pastes

Dry solids are mixed in processes associated with food, pharmaceuticals, fertilizer, tobacco, cement (qv), rubber products, ceramics (qv), soap, and many other industries. Viscous pastes are frequently handled in polymer and petroleum (qv) processes. The operations include liquid addition to solids and liquid removal from solids (drying). Mixing equipment used in such systems are uniquely designed to divide and recombine the materials to attain uniformity. Moving agitator components often scrape the walls because the material does not flow easily. The energy requirements may be very high because of the work involved in dividing, moving and shearing the material. Mixing machinery is selected according to its capacity to shear material at low speed and to tumble, wipe, smear, fold, stretch, or knead the mass to be handled. Mixers with intermeshing blades are sometimes required to keep the material from clinging unmixed to the lee side of the blade. Wiping of heat-transfer surfaces promotes addition or removal of heat. Some mixing devices break down solids in pastes and thus have the character of mills.

12.1. Dry Solids. For mixing of dry solids the mixers can be categorized according to the mixing mechanism used, eg, tumbling, convection and fiuidization.

Tumbling. Gentle mixing by a tumbling action causes materials to cascade from the top of the rotating vessel. Common types offer various vessel configurations including drum, container, *V* (Fig. 51**a**), and cone. Intake and discharge of materials in these mixers take place through an opening in the vessel end. Dry and partly dry powders, granules, and crystalline substances are readily mixed in such equipment. Intensive blending is possible with the addition of a high speed mix bar.

Convection. In these mixers an impeller operates within a static shell and particles are moved from one location to another within the bulk.

Ribbon Type. Spiral or other blade styles transfer materials from one end to the other or from both ends to the center for discharge (Fig. 51**b**). This mixer can be used for dry materials or pastes of heavy consistency. It can be

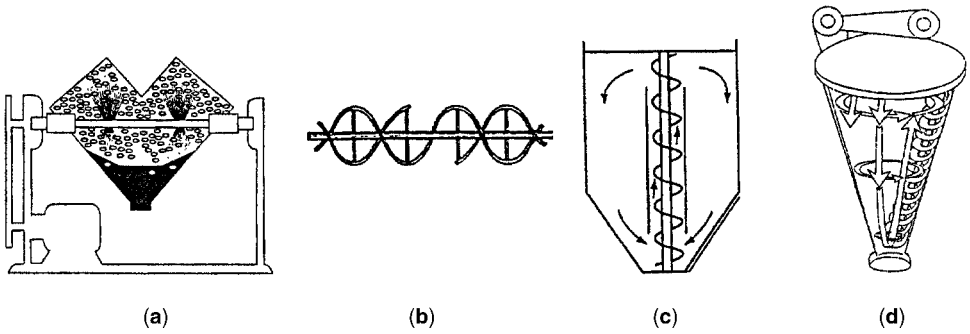

Fig. 51. Various mixer types for dry solids: (**a**) the V-mixer, (**b**) ribbon blender, (**c**) vertical screw mixer, and (**d**) Nautamix.

jacketed for heating or cooling. Blades can be smoothly contoured and highly polished when cleanliness is an important process requirement.

Spiral Elevator. Materials are moved upward by the centrally located spiral-type conveyor in a cylindrical or cone-shaped Nautamix vessel (Fig. 51**c** and **d**). Blending occurs by the downward movement at the outer walls of the vessel. The vessel serves the dual purposes of blending and storage. In these mixers, the screw impeller actively agitates only a small portion of the mixture and natural circulation is used to ensure all the mixture passes through the impeller zone. In the case of Nautamix, an Archimedian screw lifts powder from the base of a conical hopper while progressing around the hopper wall.

Paddle Type. This type is similar to the ribbon type except that interrupted flight blades or paddles transfer materials from one end to the other, or from both ends to the center for discharge. The paddle-type mixer can be used for dry materials or pastes of heavy consistency. It can be jacketed for heating or cooling.

Planetary Type. Paddles or whips of various configurations are mounted in an off-center head that moves around the central axis of a bowl or vessel. Material is mixed locally and moved inward from the bowl side, causing intermixing. This mixer handles dry materials or pastes.

Pan Type. The mulling action of this mixer is similar to the action of a mortar and pestle. Scrapers move the materials from the center and side of a pan into the path of rotating wheels where mixing takes place. The pan may be of the fixed or rotating type. Discharge is through an opening in the pan. The flow type uses rotating plows in a rotating pan to locally mix and intermix by the rotation of plows and pan, respectively.

Fluidization. Particles suspended in a gas stream behave like a liquid. They can be mixed by turbulent motion in a fluidized bed. This mixer is used for mixing and drying, or mixing and reaction. Processall horizontal mixer (Fig. 52) uses plow-shaped agitating elements extended very close to the vessel wall. These elements lift the material and thrust into free space in a pulsating or fluidized-bed action.

12.2. Pastes. For blending of viscous pastes, mixers are classified as batch or continuous. Most convection-type mixers for dry solids are also used for thick pastes.

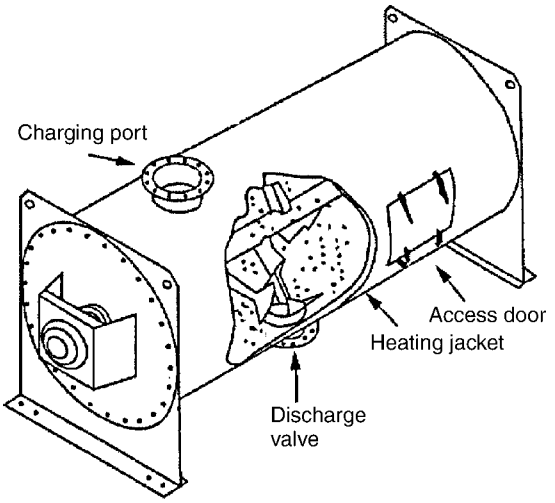

Fig. 52. Processall plow-shaped fluidizing mixer.

Batch Mixers. These mixers are preferred when batch identity must be maintained, eg, in pharmaceutical products; when frequent product changes occur and off-spec products must be minimized, eg, in dye and pigment manufacture; and when a multitude of ingredients is required with accurate additions, eg, in adhesives (qv) and caulking compounds. Also, the batch mode is best when various changes of state are involved, eg, a reaction followed by the pulling of a vacuum to drive off volatiles or when very long mixing and reacting times are required.

Change-Can Mixers. In change-can mixers one or more blades cover all regions of the can either by a planetary motion of the blades or a rotation of the can (Fig. 53**a**). The blades may be lowered into the can or the can may be raised to the mixing head. Separate cans allow the ingredients to be measured carefully before the mixing operation begins, and can be used to transport the finished batch to the next operation while the next batch is being mixed.

Stationary Tank Mixers. These are recommended when the particular advantages of the change-can mixer are not required. The agitator may be

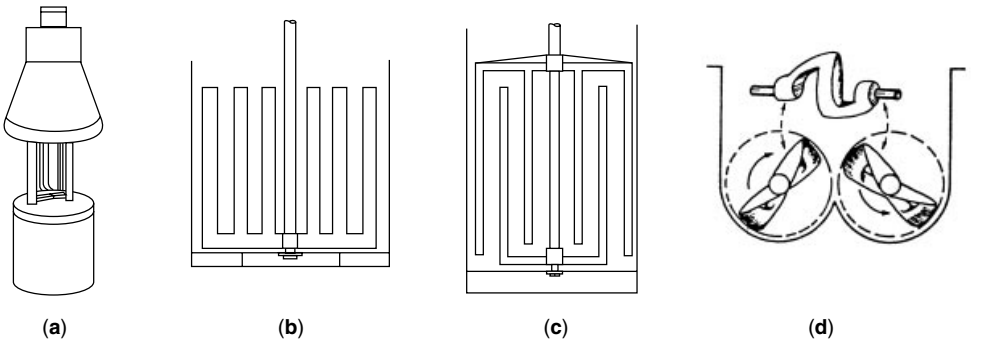

Fig. 53. Various mixer types for viscous pastes: (**a**) the change-can mixer, (**b**) rake mixer, (**c**) double-rake mixer, and (**d**) sigma-blade kneader.

particular to a specific industry, eg, the soap crutcher, or for general use as single- or double-rake mixers (Fig. 53**b** and **c**). In the latter, some part of the agitator moves in close proximity to the vessel walls or stationary bar baffles. The impeller may also consist of a single- or double-helical blade to promote top-to-bottom turnover, minimizing the amount of hardware that must be moved through the viscous mass.

Double-Arm Kneading Mixers. The material in these mixers (Fig. 53**d**) is carried by two counterrotating blades over the saddle section of a W-shaped trough. Randomness is introduced by the differences in blade speed and end-to-end mixing by differences in the length of the arms on the sigma-shaped; blades. Other blade shapes are used for specific end purposes, such as smearing or cutting edges on the blade faces. Discharge is usually by tilting the trough or by a door in the bottom of the trough. Double-arm kneading mixers are also available with a centrally located screw to discharge the contents.

Intensive Mixers. Intensive mixers such as the Banbury (Fig. 54) are similar in principle to the double-arm kneading mixers, but are capable of much higher torques. Used extensively in the rubber and plastics industries, the Banbury mixer is operated with a ram cover so that the charge can be forced into the relatively small-volume mixing zone. The largest of these mixers holds only 500 kg but is equipped with a 2000-kW motor.

Roll Mills. When dispersion is required in exceedingly viscous materials, the large surface area and small mixing volume of roll mills allow maximum shear to be maintained as the thin layer of material passing through the nip is continuously cooled. The rolls rotate at different speeds and temperatures to generate the shear force with preferential adhesion to the warmer roll.

Continuous Mixers. In most continuous mixers one or more screw or paddle rotors operate in an open or closed trough. Discharge may be restricted at the end of the trough to control holdup and degree of mixing. Some ingredients may be added stagewise along the trough or barrel. The rotors may be cored to provide additional heat-transfer area. The rotors may have interrupted flights to permit interaction with pins or baffles protruding inward from the barrel wall.

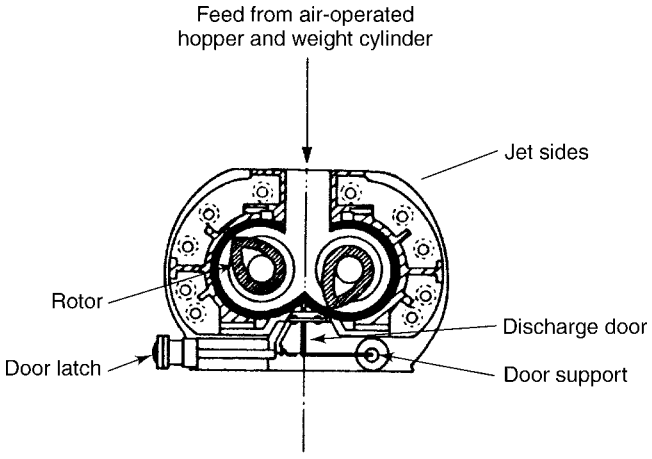

Fig. 54. Banbury mixer for viscous pastes.

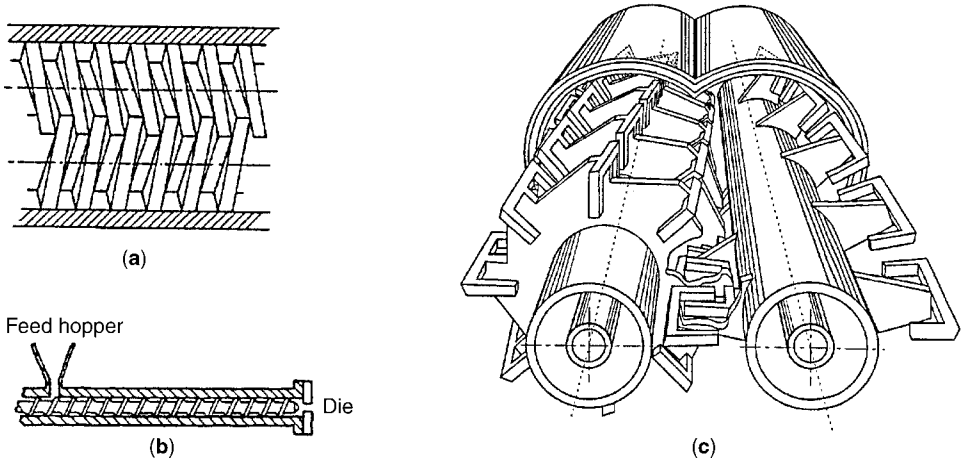

Fig. 55. Continuous mixers for paste mixing (**a**) corotating twin-screw extruder, (**b**) single screw extruder, and (**c**) LIST opposite rotating processor.

Single-Screw Extruders. These incorporate ingredients such as antioxidants (qv), stabilizers, pigments, and other fillers into plastics and elastomers (Fig. 55**b**). In order to provide a uniform distribution of these additives, the polymer is melted primarily by the work energy imparted in the extruder, rather than by heat transfer through the barrel wall. In addition to melting the polymer, the extruder is used as a melt pump to generate pressure for extrusion through a die, shaping the molten product to a specific profile, or into strands or pellets. The extruder screw drags the polymer through the barrel, generating shear between screw and barrel. In addition, some axial mixing occurs in response to a back flow along the screw channel caused by the pressure required to get through the die. Mixing in a single-screw extruder can be enhanced by interrupting the flow pattern within the screw flight channel. This can be done by variations in the screw flight channel width or depth, by causing an interchange with spiral grooves in the barrel, or by interengaging teeth.

Twin-Screw Mixers. These continuous mixers provide more radial mixing by interchange of material between the screws, rather than just acting as screw conveyors. Intermeshing corotating twin-screw mixers (Fig. 55**a**) have the additional advantage that the two rotors wipe each other as well as the barrel wall. This action eliminates any possibility of dead zones or unmixed regions. In addition to variations in screw helix angles, these mixers can be fitted with kneading paddles that interactively cause a series of compressions and expansions to increase the intensity of mixing. Such mixers are used for a variety of pastes and doughs, as well as in plastics compounding.

An opposite rotating processor (Fig. 55**c**) by LIST Company is designed for continuous processing of highly viscous and pasty or crusty material. Two parallel agitator shafts intermesh as they rotate to provide self-cleaning action with U-shaped kneading elements. The shafts rotate in a counter direction with different speeds in the ratio of 1:4. In addition to wiping action, the elements provide intensive lateral mixing. For continuolus use, a slow axial conveying is provided. The optimal fill level between 40 and 75% of the mixer volume is controlled by weir plates.

BIBLIOGRAPHY

"Mixing and Agitating" in *ECT* 1st ed., Vol. 9, pp. 133–166, by J. H. Rushton and C. W. Selheimer, Illinois Institute of Technology, and R. D. Boutros, Mixing Equipment Co., Inc.; "Mixing and Blending" in *ECT* 2nd ed., Vol. 13, pp. 577–613, by J. H. Rushton, Purdue University, and R. D. Boutros, Mixing Equipment Co., Inc.; in *ECT* 3rd ed., Vol. 15, pp. 604–637, by J. Y. Oldshue, Mixing Equipment Co., Inc., and D. B. Todd, Baker Perkins, Inc.; in *ECT* 4th ed., Vol. 16, pp. 844–887, by R. R. Hemrajani, ExxonMobil Research and Engineering Company; "Mixing and Blending" in *ECT* (online), posting date: December 4, 2000, by Ramesh R. Hemrajani, ExxonMobil Research and Engineering Company.

CITED PUBLICATIONS

1. R. R. Hemrajani, *Chem. Proc.* **50**, 22 (July 1987).
2. D. S. Dickey and J. G. Fenic, *Chem. Eng.* **83**(1), 139 (1976).
3. D. S. Dickey and R. R. Hemrajani, *Chem. Eng.* **99**(3), 82 (1992).
4. R. W. Hicks, J. R. Morton, and J. G. Fenic, *Chem. Eng.* **83**(9), 102 (1976).
5. *Handbook of Industrial Mixing, Science and Practice*, in E. L. Paul, V. A. Atiemo-Obeng and S. M. Kresta, eds., Wiley Interscience, New York, 2003.
6. Th. N. Zwietering, *CES* **8**, 244 (1958).
7. P. A. Shamlou and E. Koutsakos, *CES* **44**(3), 529 (1989).
8. R. R. Hemrajani, D. L. Smith, R. M. Koros, and B. L. Tarmy, *6th European Conference on Mixing*, Pavia, Italy, May 24, 1988.
9. D. E. Leng and G. J. Quarderer, *Chem. Eng. Commun.* **14**, 177 (1982).
10. H. J. Karam and J. C. Bellinger, *I&EC Fund.* **1**, 576 (1968).
11. A. H. P. Skelland and G. G. Ramsay, *Ind. Eng. Chem.* **26**(1), 77 (1987).
12. T. Kinugasa, K. Watanabe, T. Sonove and H. Takeuchi, Presentation at the International Symposium on L-L Two-Phase Flow, Antalya, Turkey, 1997.
13. A. W. Nienow, D. J. Wisdom, and J. C. Middleton, *2nd European Conference on Mixing*, Cambridge, U.K., Mar. 30–Apr. 1, 1977.
14. M. M. C. G. Warmoeskerken and J. M. Smith, *CES* **40**(11), 2063 (1985).
15. G. Q. Martin, *Ind. Eng. Chem. Proc. Des. Dev.* **11**(3), 397 (1972).
16. H. Fossett, *Trans. Inst. Chem. Eng.* **29**, 322 (1951).
17. E. A. Fox and V. E. Gex, *AIChE J.* **2**(4), 539 (1956).
18. M. F. Edwards and W. L. Wilkinson, *Heat Transfer to Newtonian and Non-Newtonian Fluids in Agitated Vessels*, HTFS-DR 27, Harwell, Berkshire, U.K., 1972.

GENERAL REFERENCES

Handbook of Mixing Technology, Ekato Ruhr-und Mischtechnik GmbH, Schopfheim, Germany, 1991.

N. Harnby, M. F. Edwards, and A. W. Nienow, *Mixing in the Process Industries*, Butterworths, London, 1985.

N. Harnby, *Fluid Mixing III*, The Institution of Chemical Engineers, Symposium, Series No. 108, Hemisphere Publishers, New York, 1988.

F. A. Holland and F. S. Chapman, *Liquid Mixing and Processing in Stirred Tanks*, Van Nostrand Reinhold, New York, 1966.

S. Nagata, *Mixing Principles and Applications*, John Wiley & Sons, Inc., New York, 1975.

J. Y. Oldshue, *Fluid Mixing Technology*, McGraw-Hill, Inc., New York, 1983.

Z. Sterbacek and P. Tausk, trans. K. Mayer, *Mixing in the Chemical Industry*, Pergamon Press, New York, 1965.
G. B. Tatterson, *Fluid Mixing and Gas Dispersion in Agitated Tanks*, McGraw-Hill, Inc., New York, 1991.
V. W. Uhl and J. B. Gray, *Mixing-Theory and Practice*, Vols. I & II, Academic Press, Inc., 1966–1967; V. W. Uhl and J. A. Von Essen, Vol. III, 1986.
J. J. Ulbrecht and G. K. Patterson, *Mixing of Liquids by Mechanical Agitation*, Gordon & Breach Science Publishers, New York, 1985.

General Concepts

R. R. Corpstein, R. A. Dove, and D. S. Dickey, *CEP* **75**(2), 66 (1979).
D. S. Dickey, *CEP* **87**(12), 22 (1991).
J. B. Joshi, A. B. Pandit, and M. M. Sharma, *CES* **37**(6), 813 (1982).
Y. Kawase and M. Moo-Young, *Chem. Eng. J.* **43**, B19 (1990).
D. E. Leng, *CEP* **87**(6), 23 (1991).
K. W. Norwood and A. B. Metzner, *AIChE J.* **6**(3), 432 (1960).
J. H. Rushton, E. W. Costich, and H. J. Everett, *CEP* **46**(8), 395 (1950).
G. B. Tatterson, R. S. Brodkey, and R. V. Calabrese, *CEP* **87**(6), 45 (1991).
V. W. Uhl, *Chem. Proc.* **47**, 26 (1984).

Liquid Blending

J. B. Fasano and W. R. Penney, *CEP* **87**(12), 46 (1991).
J. B. Fasano and W. R. Penney, *CEP* **87**(10), 56 (1991).
M. C. Jo, W. R. Penney, and J. B. Fasano, *1993 AIChE Annual Meeting*, St. Louis, Mo.
S. J. Khang and O. Levenspiel, *Chem. Eng.* **83**(10), 141 (1976).
H. Kramers, G. M. Baars, and W. H. Knoll, *CES* **2**, 35 (1953).
J. Y. Oldshue, H. E. Hirschland, and A. T. Gretton, *CEP* **52**(11), 481 (1956).
R. K. Grenville, Ph.D. Dissertation, Cranfield Institute of Technology, Cranfield, England, 1992.

Solid–Liquid

M. Bohnet and G. Niesmak, *Ger. Chem. Eng.* **3**, 57 (1980).
L. E. Gates, J. R. Morton, and P. L. Fondy, *Chem. Eng.* **83**(11), 144 (1976).
T. Hobler and J. Zablocki, *Chem. Tech. (Leipzig)* **18**, 650 (1966).
A. W. Nienow, *CES* **23**, 1453 (1968).
G. E. H. Joosten, J. G. M. Schilder, and A. M. Broere, *Trans. Inst. Chem. Eng.* **55**, 220 (1977).

Liquid–Liquid

M. M. Clark, *CES* **43**(3), 671 (1988).
J. C. Godfrey, F. I. N. Obi, and R. N. Reeve, *CEP* **85**(12), 61 (1989).
R. R. Hemrajani, *5th European Conference on Mixing*, Wurzburg, June 10–12, 1985.
W. J. McManamey, *CES* **34**, 432 (1979).
R. Shinnar and J. M. Church, *Ind. Eng. Chem.* **53**, 479 (1961).
V. G. Trice and W. A. Rodger, *AIChE J.* **2**(2), 205 (1956).

J. W. Van Heuven and J. C. Hoevenaar, *Proceedings of 4th European Symposium on Chemical Reaction Engineering*, Brussels, 1968.
T. Vermeulen, G. M. Williams, and G. E. Langlois, *CEP* **51**(2), 85-F (1955).
R. V. Calabrese, T. P. K. Chang and P. T. Dang, *AIChEJ* **32**(4), 657 (1986).

Gas–Liquid

R. W. Hicks and L. E. Gates, *Chem. Eng.* **83**(7), 141 (1976).
V. B. Rewatkar and J. B. Joshi, *Can. J. Chem. Eng.* **71**, 278 (1993).
C. D. Rielly, G. M. Evans, J. F. Davidson, and K. J. Carpenter, *CES* **47**, 3395 (1992).

Jet Mixing

J. H. Rushton and J. Y. Oldshue, *CEP* **49**(4), 161 (1953).
R. K. Grenville and J. N. Tilton, *Trans. Inst. Chem. Eng.* **74**, 390 (1996).

Heat Transfer

M. F. Edwards and W. L. Wilkinson, *Heat Transfer to Newtonian and Non-Newtonian Fluids in Agitated Vessels*, HTFS-DR 27, Harwell, 1972.
A. Niedzielska and Cz. Kuncewicz, 5th Inbternational Sympsuin on Mixing in Industrial Processes, June 1–4 2004, Seville, Spain.

RAMESH R. HEMRAJANI
ExxonMobil Research and Engineering Company